

Uncertainty quantification and global sensitivity analysis of continuous distillation considering the interaction of parameter uncertainty with feed variability.

José M. Gozálvéz-Zafrilla ^{a*}, J. Carlos García-Díaz ^b, Asunción Santafé-Moros ^a

^a Research Institute for Industrial, Radiophysical and Environmental Safety (ISIRYM), Universitat Politècnica de València, Valencia (Spain)

^b Department of Applied Statistics, Operational Research and Quality, Universitat Politècnica de València, Valencia (Spain)

Abstract

In this work, uncertainty and sensitivity analyses were applied to study the joint effects of model parameter uncertainty, feed and operation variability on the response of a computational code for continuous distillation of methanol–water. First, model parameter uncertainty (liquid–vapour equilibrium, enthalpy and tray efficiency) was characterised using existing experimental data. Afterwards, three tower configurations working at two operational modes (fixed product composition and fixed operation conditions) were studied at three feed variability levels. Morris analysis revealed the high importance of the VLE and efficiency-related factors. Sobol sensitivity analysis determined with more precision the sensitivity of the response to the parameters and detected non-linear effects and interactions. The Monte Carlo propagation method allowed obtaining the uncertainty margins as a function of feed variability. The results showed high impact of the model parameter uncertainty and encourage the use of the methods shown to obtain robust designs and quantify simulation accuracy.

Keywords: distillation, uncertainty, sensitivity, Morris analysis, Sobol method

1 Introduction

Continuous distillation towers process large amounts of chemical product and consume a large share of the energy used in the chemical industry (Resetarits and Lockett, 2003; Shahandeh et al., 2015). The preliminary design of tray distillation towers aims to obtain their optimal topology (number of stages and feed stage) and operation variables (reflux ratio, reboiler and condenser heat duties) to meet product specifications. Distillation calculations require modelling of the component separation, which is mainly accomplished by the vapour–liquid equilibrium model (VLE), enthalpy model and the use of tray efficiency correlations. McCabe–Thiele and Ponchon–Savarit are well known methods for the design of distillation towers, the latter being more rigorous, as it considers the energy balance equations in the trays. Both methods are applied for a previously defined reflux ratio. The value of the reflux ratio can later be optimised looking for a reasonable balance between capital cost and energy consumption. For a specified tower configuration, a simulation based on the same model equations used in these methods can be used to obtain the tower performance.

The design and simulation of distillation columns is usually carried out by consideration of constant feed characteristics and fixed model parameters. Nevertheless, model parameters are subject to a certain degree of uncertainty for different reasons, such as lack of accuracy of the experimental data used to fit them or because the model is not sufficiently accurate to represent the physical behaviour over a broad range of conditions. Therefore, the uncertainty in the model parameters and modelling accuracy imply uncertainty of the model response even for deterministic inputs.

The correlations of phase equilibrium can potentially be the most important source of property uncertainties in process design (Mathias, 2016). These uncertainties come from the lack of exactitude of the models but also from the estimation of the model parameters from experimental data sets (Ulas et al., 2005). Therefore, the uncertainty of parameters fitted from experimental data should be propagated through the equilibrium model.

Efficiency prediction of crossflow trays is still not completely satisfactory for rigorous design (Couper et al., 2010). However, there is continuous progress, and more sophisticated methods are being developed to predict point efficiency from local conditions. Overall tray efficiency E_{MV} (Murphree efficiency) is obtained by conversion of point efficiencies based on hydraulic considerations. As the Murphree efficiency relates the input and output streams through equilibrium, the combined effect of the equilibrium and efficiency uncertainties can have great impact on the global uncertainty. (Lashmet and Szczepanski, 1974) performed an uncertainty study on binary distillation columns using bubble cap-trays. They demonstrate that overdesign factors for the number of stages up to 1.25 were needed to reach 90% confidence if the AIChE method of Murphree efficiency estimation is used. Besides the efficiency uncertainty associated with the correlations used, feed impurities can have a great influence. (Yang et al., 2003) studied tray efficiency in methanol–water distillation. They compared efficiencies, obtained working at the same operating conditions, of mixtures of laboratory-grade components and two samples of industrial origin. For some conditions, differences in efficiency of up to 0.1 were obtained. They attributed these differences mainly to the high influence of foaming effects on methanol–water mixtures.

On the other hand, feed variability can be an important source of uncertainty in distillation systems, especially when the feed comes from different processes and sources (Enagandula and Riggs, 2006; Henrion and Möller, 2003; Li et al., 2002). The feed of a distillation tower can be subject to important variations in flow, energy state or composition because of the different nature of the feeds used and the stochastic behaviour of previous processes. (Henrion and Möller, 2003) identified two types of feed uncertainty: inputs from non-overlapping external processes with different starting times and inputs from the superposition of many independent elementary inflows (Gaussian model). Feed variability can be reduced by using accumulation tanks and heat exchangers with efficient controls, but it cannot be completely suppressed. That is the case for complex mixtures such as those processed by the petroleum industry where important variations in flow and composition can arise (Sánchez et al., 2007). In the case of the industrial methanol–water separation, (Li et al., 2002) showed a typical case in which flow varies up to $\pm 7\%$ and composition around $\pm 20\%$.

The joint effect of the mentioned uncertainty sources implies an important uncertainty of the system output, which is better characterised by a probability distribution rather than by a unique deterministic value. The knowledge of uncertainty effects on the model output can help to accomplish robust designs and to select operating conditions that minimise the need for control actions. Using this methodology it is possible to determine the worst-case variability of a process variable at a given probability to have minimum operational and economic requirements (Aneesh et al., 2016; Ricardez-Sandoval, 2012). However, in spite of the benefits that uncertainty analysis can provide, it is not a routine element in industrial practice (Mathias, 2016).

The application of uncertainty and sensitivity analysis requires a model or computational code $f(X)$ to describe the system in terms of a set of input variables of random nature given by the model input random vector X . Consequently, the vector of responses of the model, $Y = f(X)$, will be random. The fundamental objective of the analysis of the responses focuses on the study of their probabilistic distribution and the quantification of the variability transmitted from the inputs through the model corresponding to each input. The main stages of this process are: *i*) definition of the model or computational code of the system, *ii*) quantification of the uncertainty sources, *iii*) propagation of the uncertainty through the computational code, and *iv*) uncertainty and sensitivity analysis.

The uncertainty analysis focuses on quantifying the uncertainty in the Y response of the model. The uncertainty propagated through the computational code turns up in the variability of the response or output and is measured by the variance in Y .

(Saltelli et al., 2004) defined global sensitivity analysis as the study of how the uncertainty in the model response (output) can be attributed to the different sources of uncertainty in the model inputs.

The Morris method (Morris, 1991) is a screening strategy whose objective is to explore which input variables in a computational model can be classified into factors that have a negligible, linear and additive, or non-linear effect or interaction with other factors on each model response. The method yields the relative importance of the different input factors on the response or output of the model. The Sobol sensitivity analysis, based on the decomposition of the variance in the output of the computational model, has the objective of determining the different fractions of the final variability that can be assigned to each of the

inputs of the model and to the possible interaction between two or more inputs (Sobol, 1993). This method allows detection of the sensitivity of the model in its entirety, considering all input variables. Similarly, it allows dealing with non-linear response variables, as well as measuring the effect of interactions between inputs in non-additive systems. The details of both methods are shown in Appendix A.

The aim of this work was to study the joint effect of model uncertainty and feed variability on the uncertainty response of a computational code for continuous distillation considering different tower configurations. The case of study was the methanol–water separation in a continuous distillation tower of sieve trays. The computational code was used to obtain the tower configurations able to meet previously stated product specifications in the typical range of reflux-to-minimum reflux ratios. Afterwards, three tower configurations were selected as representative cases of low, medium and high reflux ratios.

Uncertainty and sensitivity analyses were applied to each tower configuration for two operational modes. In the first operational mode, the composition of both product streams was specified at reference values and the necessary operating conditions of reflux and reboiler heat duty were the responses studied. This situation reflects the uncertainty in the control set point of the distillation tower. In the second operational mode, the operating conditions were set at reference values and the main responses studied were the compositions of both product streams. This situation would reflect the direct impact of the uncertainty on the output streams in the case of a non-controlled tower.

In the Material and Methods section, we firstly describe the study case, and the model equations and the iterative calculation procedure used in the computational code. Secondly, we show the methodology of fitting and uncertainty characterisation of the model parameters followed by the procedure of uncertainty and sensitivity analysis.

In the Results and Discussion section, we firstly show the determination of the feasible tower configurations. Second, we show the results of the Morris analysis for the three tower configurations selected at three levels of feed uncertainty and the results obtained by the Sobol method corresponding to the medium-reflux-ratio tower design. Finally, the results of the uncertainty analysis show the uncertainty margins for the two operational modes as a function of the level of feed variability for the selected tower configurations.

2 Materials and Methods

2.1 Model description

The simulation algorithm was built following a multi-compartment description of the distillation tower in which each stage is considered as a lumped compartment. Balance equations for the total molar flow (Eq. (1), molar flows of key component (Eq. (2) and enthalpy flows (Eq. (3) are applied to each stage n . The right-hand side of Eqs. 1–3 is zero except for the feed tray and the reboiler. The vapour composition in equilibrium with the liquid composition and the corresponding temperature is obtained from the equilibrium

model. The composition of the vapour fractions at each stage is related to the fraction corresponding to the equilibrium y_n^* through the Murphree's vapour tray efficiency $E_{MV,n}$ (Eq. (4)).

$$-L_{n-1} + V_n + L_n - V_{n+1} = F_n \quad (1)$$

$$-L_{n-1} x_{n-1} + V_n y_n + L_n x_n - V_{n+1} y_{n+1} = F_n z_{F_n} \quad (2)$$

$$-L_{n-1} h_{L_{n-1}} + V_n h_{V_n} + L_n h_{L_n} - V_{n+1} h_{V_{n+1}} = F_n h_{F_n} + q_n \quad (3)$$

$$E_{MV,n} = \frac{y_n - y_{n+1}}{y_n^* - y_{n+1}} \quad (4)$$

The VLE was modelled with the non-random two-liquid model (NRTL), which has been successfully applied to distillation of alcohol–water systems (Kurihara et al., 1993; Puentes et al., 2018; Soujanya et al., 2016, 2010; Yang et al., 2011). The NRTL model correlates the activity coefficients with the molar fractions in the liquid phase. In the case of a binary mixture of components 1 and 2, the equations of the liquid phase activity coefficients for the NRTL model are given by Eqs. (5) and (6):

$$\ln \gamma_1 = x_2^2 \cdot \left[\tau_{2,1} \cdot \left(\frac{G_{2,1}}{x_1 + G_{2,1} x_2} \right)^2 + \frac{\tau_{1,2}}{G_{1,2}} \cdot \left(\frac{G_{1,2}}{x_2 + G_{1,2} x_1} \right)^2 \right] \quad (5)$$

$$\ln \gamma_2 = x_1^2 \cdot \left[\tau_{1,2} \cdot \left(\frac{G_{1,2}}{x_2 + G_{1,2} x_1} \right)^2 + \frac{\tau_{2,1}}{G_{2,1}} \cdot \left(\frac{G_{2,1}}{x_1 + G_{2,1} x_2} \right)^2 \right] \quad (6)$$

In these equations, the groups $G_{1,2}$, $G_{2,1}$, $\tau_{1,2}$ and $\tau_{2,1}$ are functions of the three binary parameters of the model (α , Δg_{12} , Δg_{21}) expressed in Eqs. (7–(10):

$$G_{1,2} = \exp(-\alpha \tau_{1,2}) \quad (7)$$

$$G_{2,1} = \exp(-\alpha \tau_{2,1}) \quad (8)$$

$$\tau_{1,2} = \frac{\Delta g_{1,2}}{R_g T} \quad (9)$$

$$\tau_{2,1} = \frac{\Delta g_{2,1}}{R_g T} \quad (10)$$

Enthalpy correlations were used to determine the enthalpy of the liquid stream and the vapour stream as a function of their composition.

Murphree tray efficiency depends on tray geometry, operating conditions and stream properties of the streams in the tray. It was calculated using a sieve tray model developed recently by (Syeda et al., 2007). The estimation of the jetting fraction of the model was improved with the modification recommended by (Vennavelli et al., 2012).

2.2 Calculation procedure

2.2.1 Algorithm for the determination of feasible configurations

An algorithm to obtain the tower configurations able to meet specified compositions in both product streams was built using the model equations of the previous section. The calculation procedure was quite similar to the Ponchon–Savarit method (Treybal, 1980) but considering tray efficiency. The algorithm was implemented in Matlab 2019a.

2.2.2 Iterative calculation for tower operating at fixed product compositions.

For a tower of specified configuration, this calculation procedure was intended to obtain the reflux ratio and reboiler heat duty able to meet the composition specifications at the top and bottom output streams. Previously, the molar flows of the product streams, were obtained using mass balances. The calculation procedure (Figure 1) started by guessing the reflux ratio R . The condenser and reboiler heat duties were obtained by applying balances to the condenser and the whole tower respectively. As in the Ponchon–Savarit method, pole coordinates h_{AD} and h_{AW} representing the composition and enthalpy state of the top and bottom of the tower were determined. Next, two calculation sequences were started: from top to feed location and from bottom to feed location. Each calculation sequence subsequently involved the use of the balance equations for total moles, energy and component balance, the VLE model and the tray efficiency model. The results of molar flow, composition and enthalpy of the streams over the feed location obtained in both calculation sequences were used to estimate the relative error of the component balance of the calculation (CBE). The value of R was modified to reduce the relative error under a specified tolerance.

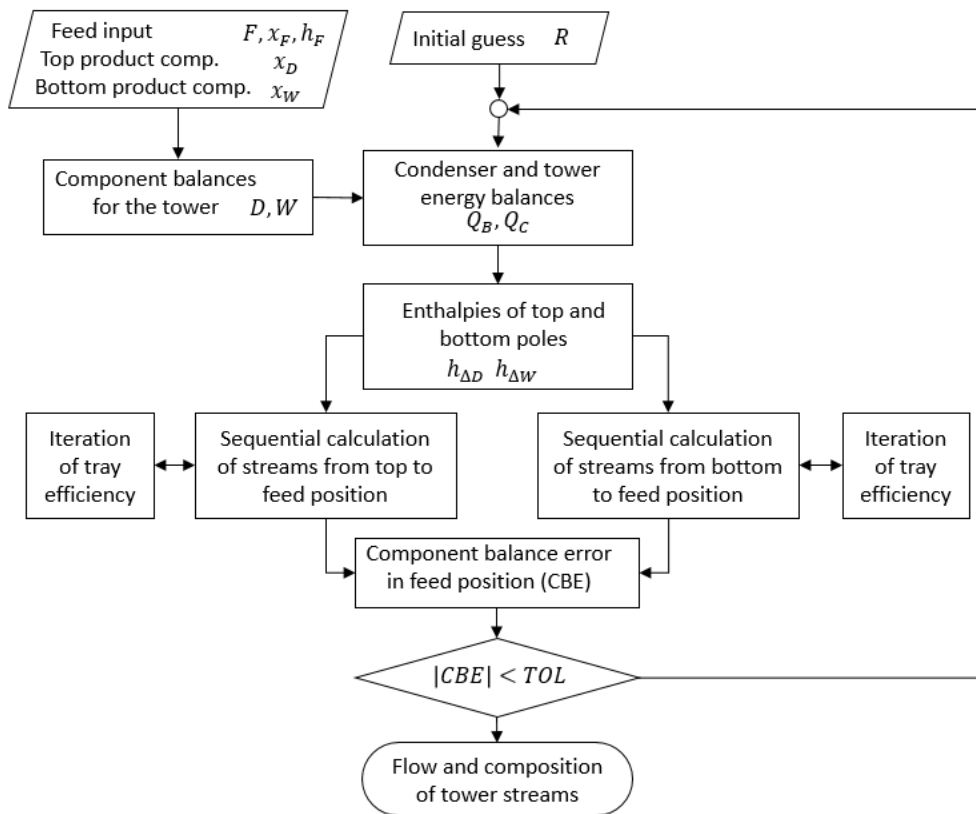


Figure 1. Iterative procedure to simulate tower operating at fixed output stream compositions x_D and x_W .

2.2.3 Iterative calculation for tower operating at fixed reflux ratio and reboiler heat duty

In this case, the calculation procedure was intended to obtain the product compositions given the tower configuration, reflux ratio and reboiler heat duty. The calculation procedure started by guessing the top product composition x_D . The molar flows of the product streams, the bottom composition and the heat duty to be retired from the condenser were obtained by applying balances to the whole tower and to the condenser. Afterwards, a similar procedure to that used in 2.2.2 was applied to estimate the component balance error of the calculation (CBE). The value of x_D was modified to reduce the relative error of the calculation under a specified tolerance.

2.3 Case study

The case study was defined to illustrate the application of the uncertainty and sensitivity methodology to a continuous distillation process. The methanol–water system was selected because of its industrial relevance (Abolpour et al., 2013; Biddulph and Kalbassi, 1988; Shahandeh et al., 2015; Yang et al., 2003). Table 1 shows the deterministic values of the specific feed stream used and the targeted compositions of the top and bottom products in terms of the molar fraction of the light key component (methanol). Table 1 also shows the tray geometry used, which was obtained using the methodology of design detailed in (Treybal,

1980). The sieve tray dimensions were set by considering previous calculations to determine approximate ranges for the internal flows.

Table 1. Deterministic reference values, specifications and tray dimensions of the case study

Feed characteristics	Flow	$F = 100$ kmol/h
	Methanol fraction	$z_F = 0.5$
	Vapour fraction	$f_v = 0.5$
Methanol fraction specification	Top product	$x_{Dref} = 0.95$
	Bottom product	$x_{Wref} = 0.05$
Sieve tray dimensions ⁽¹⁾	Diameter	0.9 m
	Weir height	0.05 m
	Weir length	0.63 m
	Hole diameter	4.5 mm
	Pitch of holes	13.5 mm

A set of feasible tower topologies was obtained by varying the ratio of the reflux-to-minimum reflux ratio (R/R_{min}) in the range 1.1–1.5, which is the practical range for distillation columns based on cost estimation (Seader et al., 2011). The reflux values were set according to the aforementioned range and the configurations (number of trays and feed location) with higher approach to the product composition were selected. As Ponchon–Savarit is a design method, the composition requirements for both product streams are not met for a definite tower topology for the calculated reflux ratio and reboiler heat duty. Therefore, for each tower configuration, the reflux ratio and reboiler heat duty were adjusted to meet product requirements using the iterative procedure defined in 2.2.2. For the subsequent uncertainty and sensitivity analyses, three tower configurations, corresponding to the lowest, medium and highest reflux in the range, were selected.

2.4 Fitting and uncertainty characterisation of model parameters

2.4.1 Vapour–liquid equilibrium model

The model parameters were fitted to activity coefficients calculated from experimental data (Eq. (11)). We used nine different sets of experimental VLE data of the methanol–water system from different authors and accessible databases (CHERIC (Chemical Engineering and Materials Research Information Center), n.d.; Dalager, 1969; Gmehling et al., 1977; Kurihara et al., 1993; Seader et al., 2011; Verhoeve and De Schepper, 1973; Yang et al., 2011). The objective function used was the relative least-squares (Eq. (12) recommended by (Gau et al., 2000) to determine the vector of NRTL parameters $s = (\alpha, \Delta g_{12}, \Delta g_{21})$ for components

methanol ($i = 1$) and water ($i = 2$) and N_{exp} experimental points. Minimisation of the error function was carried out using simulated annealing and continuation with the Nelder–Mead method.

$$\gamma_{i,k,exp} = \frac{y_{i,k,exp} P_t}{x_{i,k,exp} P_{vap,i}(T_{k,exp})} \quad (11)$$

$$\Phi(\vec{s}) = \sum_{i=1}^2 \sum_{k=1}^{N_{exp}} \left(\frac{\gamma_{i,k,exp} - \gamma_{i,k,calc}(T_{k,exp}, x_k, \vec{s})}{\gamma_{i,k,exp}} \right)^2 \quad (12)$$

The uncertainty and sensitivity analyses require obtaining appropriate uncertainty margins for the parameters to express the variability in the experimental data. Uncertainty can be quantified by looking at the difference between the fitted model and experimental data. (Mathias, 2014) developed a method based upon the Margules equation for the perturbation of any activity coefficient model. Using this method, the logarithm of the activity coefficient is expressed as the sum of the deterministic value calculated by the model and a contribution due to uncertainty (Eq. (13)). This contribution is obtained from the value of the model activity coefficient and a perturbation parameter δ_i (Eq. (14))

$$\ln(\gamma_i) = \ln(\gamma_i^m) + \ln(\gamma_i^p) \quad (13)$$

$$\ln(\gamma_i^p) = \delta_i (1 - x_i)^2 \frac{|\ln(\gamma_i^m)|}{(1 - x_i)^2 + |\ln(\gamma_i^m)|} \quad (14)$$

The VLE data should be especially evaluated in the low-concentration regions (Mathias, 2017), as these regions are the most critical for the distillation process as they involve a greater number of stages. Therefore, the initial ranges for each perturbation parameter were selected to include the experimental data of activity coefficients in the low-concentration region for each compound. Afterwards, as the relative volatility is the most relevant variable from the point of view of separation, the ranges for the perturbation parameters were refined by looking at this parameter. The criterion used was that the region defined by the perturbation range should include 95% of the relative volatility values calculated from experimental data.

2.4.2 Enthalpy correlations

Three different data sources were found for the enthalpy of the liquid and the saturated vapour of methanol–water mixtures (Dunlop, 1948; Katayama, 1962; Treybal, 1980) and for the excess enthalpy of liquid methanol–water mixtures (Abello, 1973; Benjamin and Benson, 1963; Zhong et al., 2008). Polynomial expressions were fitted for the saturated liquid and vapour using their respective whole data sets. The excess enthalpy data of liquid methanol mixtures were used as additional data to determine the variability of the experimental data of liquid mixtures. Enthalpy uncertainty factors were defined as the ratio of the variable under uncertainty to the correlation value and considered as uniform distributions. Their range was set to include all the experimental enthalpy data.

2.4.3 Tray efficiency

Pure gas and liquid properties were obtained from DIPPR correlations (DDBST GmbH, n.d.). For the gas mixture, diffusion coefficients and mixture viscosities were obtained using the correlations of (Fuller et al., 1966) and (Buddenberg and Wilke, 1949), respectively. For the liquid mixture, a specific volume correlation corrected with a Grundberg constant was fitted to data from (Kubota et al., 1980), the diffusion coefficient was modelled by the Wilke–Chang equation, the model for surface tension was based on the Wilson equation (Chunxi et al., 2000) and fitted to data from (Khosharay et al., 2017; Vazquez et al., 1995), and the liquid viscosity correlation (Katti et al., 2008) was tested with data from (Guettari and Gharbi, 2011; Kubota et al., 1980; Marczak et al., 2012).

The performance of an efficiency model is assessed through parity plots of predicted point efficiencies versus point efficiencies that have been estimated from experimental Murphree efficiencies. Several authors provide uncertainty limits for the ratio of observed point efficiency to model efficiency (Bassat et al., 2005; J Antonio Garcia and Fair, 2000; J.A. Garcia and Fair, 2000; Luo et al., 2012; Saghatoleslami et al., 2011; Syeda et al., 2007; Vennavelli et al., 2014). Similar uncertainty limits are expected for the ratio of observed tray efficiencies to model tray efficiencies (Eq. (15) when the same correlation to relate overall tray and sieve point efficiencies is used.

$$UF_E = \frac{E_{MV,obs}}{E_{MV,model}} \quad (15)$$

As a conservative approach, the uncertainty factor was assumed to be uniformly distributed and its range was widened by multiplying it by a safety factor. During each Monte Carlo run, the uncertainty factor was computed and the value obtained applied to modify the efficiency profile calculated using the efficiency model.

2.5 Uncertainty and sensitivity analysis

The uncertainty and sensitivity analysis were applied to the tower configurations corresponding to low, medium and high reflux selected from the set of feasible configurations.

Feed variability was modelled by multiplying the reference values of flow, composition and enthalpy by uncertainty factors in the ranges $[1 - FV, 1 + FV]$ where $\pm FV$ refers the feed variability level. Uniform and independent distributions for the feed uncertainties were assumed as a conservative criterion. This assumption encompasses the two types of feed variability mentioned in the Introduction section and also makes the screening method used readily applicable. Three levels of variability were used in the uncertainty and sensitivity analysis: $\pm 3\%$, $\pm 6\%$, and $\pm 9\%$. Higher values of feed variability showed lack of convergence in many calculation runs.

Model parameter uncertainty was modelled also assuming uniform and independent distributions for the uncertainty parameters defined in Section 2.4.

To analyse the interaction of model uncertainty and input variability, each tower configuration was studied in two operational modes:

- I. Fixed output stream composition.
- II. Fixed reflux ratio and reboiler heat duty.

The first study represents the effect on the operating point uncertainty of the joint effects of the parameter uncertainty and feed variability for a controlled tower. Methanol fractions of the top and the bottom products were fixed to the reference values shown in Table 1, and the values of the operating parameters reflux ratio and reboiler heat duty that met the specifications were calculated. The main responses studied were the ratios of the reflux and reboiler heat duty obtained under variability to their respective reference values ($R^* = R/R_{det}$ and $Q_B^* = Q_B/Q_{Bdet}$). The reference values corresponded to the deterministic solution of the model obtained for each tower configuration studied (Table 2).

The second study represents the effect of the uncertainty on the product quality for a non-controlled tower. The operation parameters were fixed to the reference values obtained for each tower configuration (Table 2), and the output stream compositions were calculated. In this case, the main responses were the methanol fractions (x_D, x_W).

In both studies the ratios of the output flows to their respective reference values ($D^* = D/D_{det}$ and $W^* = W/W_{det}$) were also analysed. The values of the reference output flows D_{det} and W_{det} were equal to 50 kmol/h for the reference feed and product composition requirements. The use of relative values rather than the direct response seeks to arrive at a similar scale in the graphical results of the sensitivity analyses performed.

The uncertainty and sensitivity calculations were carried out using Matlab 2019a and R-software (3.6 version) (R Core Team, 2018). The analysis implied the generation of a design matrix of input combinations, the calculation of the corresponding runs with the computational model, and the analysis with the statistical software. Figure 2 shows the procedure used. It can be seen how the interoperability of both software was achieved thanks to the use of CSV files.

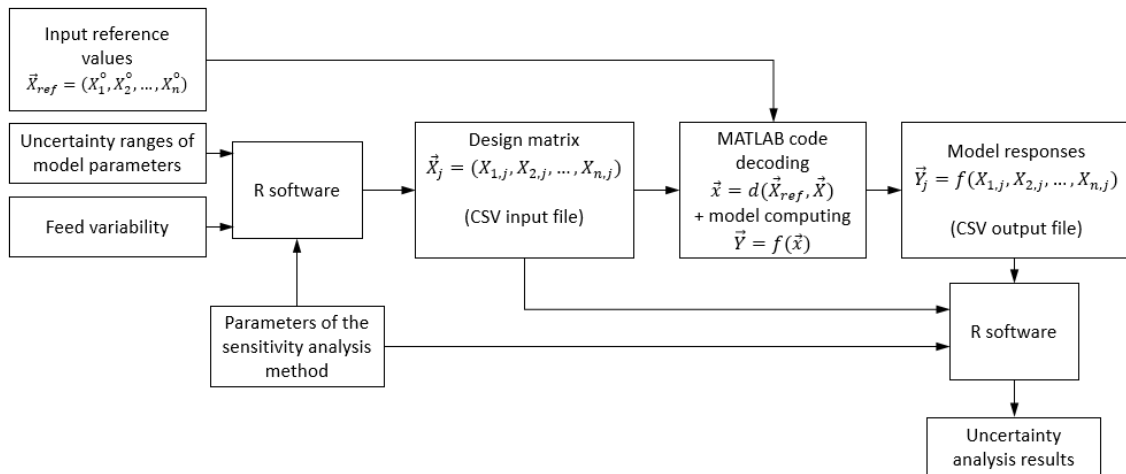


Figure 2. Workflow diagram for the uncertainty and sensitivity analysis using the computational code in Matlab and the statistical analysis software (R-software).

2.5.1 Morris screening

Morris analysis (Morris, 1991) was applied to the three selected tower configurations as a screening method useful in determining the relative importance of the uncertainty factors. The implementation of the Morris method in the sensitivity package of the R-software used space-filling optimisation (Campolongo et al., 2007) and simplex-based design (Pujol, 2009). The selected design was of type OAT (One-at-a-Time design) with 10 repetitions and four levels. As recommended by Morris, the grid jump used for computing the elementary effects was set to be half the number of levels. The design table was composed of 90 combinations of the eight coded uncertainty factors. After decoding the uncertainty factors, the corresponding responses to each factor combination were calculated using the Matlab model. The response matrices obtained were analysed further and yielded the statistics σ and μ^* for each uncertainty factor (see Appendix A).

2.5.2 Sobol sensitivity analysis

Sobol sensitivity analysis (Sobol, 1993) based on variance decomposition was applied to determine the contribution to the global uncertainty of each uncertainty factor. The analysis was only applied to the tower configuration T3 and the intermediate feed variability level as a representative central case. The Sobol analysis was applied to the whole set of uncertainty factors and for a subset of uncertainty factors, discarding the less relevant ones according to the results of the Morris analysis (see Appendix A). The analysis was performed in R-software using a subroutine based on the improved formulas of (Jansen, 1999) and (Saltelli et al., 2010a). The method used two random samples of 1000 combinations of the uncertainty factors and 100 bootstrap replicates with a confidence level of 0.95 for bootstrap confidence intervals. The resulting design matrix had a total of 10,000 combinations of factors.

2.5.3 Uncertainty analysis

The Montecarlo propagation method was used to estimate the uncertainty margins of the model responses at 95% of probability content and the median values for the three tower configurations selected. One thousand combinations of the uncertainty factors were generated and the corresponding responses further obtained by the model for the situations of specified product composition and given operating conditions. In this analysis, besides the previously used levels of feed variability, an additional calculation with no input feed variability was performed.

3 Results and Discussion

3.1 Deterministic calculation of feasible configurations

Prior to the application of the Ponchon–Savarit method considering tray efficiency, a minimum reflux ratio of $R_{min} = 0.832$ was obtained for the composition specification of the top product.

The configurations obtained, together with their corresponding deterministic operating conditions, are shown in Table 2. As mentioned before, the tower configurations obtained are representative of different ratios of energy cost to depreciation cost (Abolpour et al., 2013). According to this, the tower configurations, T1, T3 and T5 were selected for the uncertainty and sensitivity analysis, T1 and T5 as the lowest and highest reflux of the range and T3 as a typical intermediate situation.

Table 2. Feasible tower configurations and operation specifications obtained in design mode for the base case specifications

Tower id.	Tower configuration		Deterministic values of operating conditions		
	No. of stages	Feed position	Reflux ratio R_{det}	R_{det}/R_{min}	Reboiler heat duty, $Q_{B,det}$ (MJ/h)
T1	14	10	0.938	1.127	1626
T2	13	9	0.984	1.183	1710
T3	12	9	1.023	1.230	1779
T4	11	8	1.115	1.340	1943
T5	10	8	1.247	1.499	2179

3.2 Fitting and uncertainty characterisation of model parameters

In the case of the VLE model, the fitted NRTL parameters were $\Delta g_{12} = -77.16$ J/mol, $\Delta g_{21} = 393.8$ J/mol and $\alpha = 0.3876$. The ranges obtained for the perturbation parameter for methanol and water activity coefficients were $\delta_1 = [-0.28, 0.28]$ and $\delta_2 = [-0.45, 0.47]$, respectively. Figure 3 shows how the space of variability defined by these uncertainty margins covered the variability of the experimental data of relative volatility with good approximation even in the low-concentration regions.

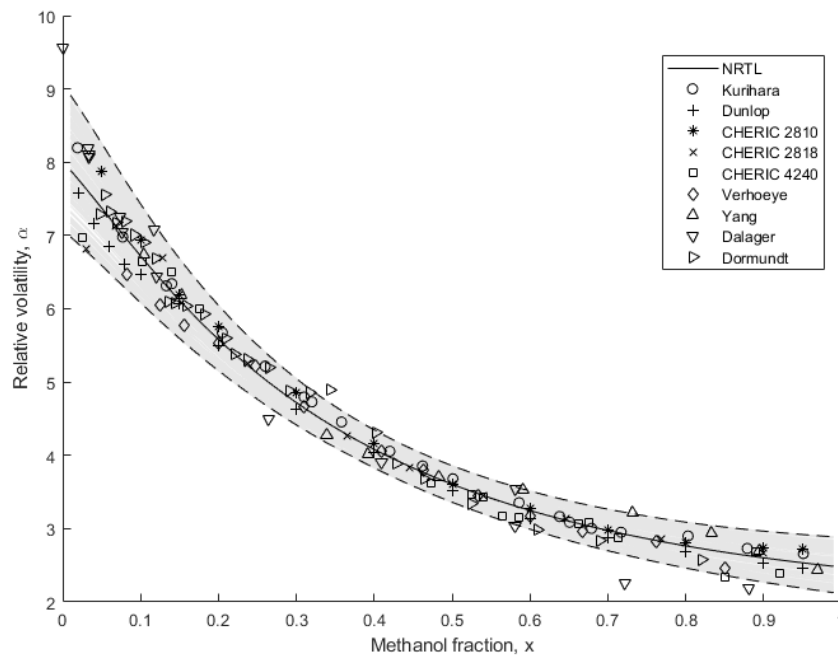


Figure 3. Validation of the uncertainty margins for the activity coefficient parameters with the experimental values of relative volatility of methanol–water using literature data (CHERIC (Chemical Engineering and Materials Research Information Center), n.d.; Dalager, 1969; DDBST, n.d.; Dunlop, 1948; Kurihara et al., 1993; Verhoeye and De Schepper, 1973; Yang et al., 2003).

The fitted polynomial expressions for the saturated liquid and vapour (kJ/kmol) are shown in Eqs. (16) and (17).

$$h_L(x) = 7473.44 - 7337.66 \cdot x + 9428.61 \cdot x^2 - 4121.42 \cdot x^3 \quad (16)$$

$$h_V(y) = 48192.6 - 7249.78 \cdot y + 982.869 \cdot y^2 - 1209.04 \cdot y^3 \quad (17)$$

In this case, the enthalpy uncertainty could not be characterised as rigorously as the equilibrium uncertainty because of the few experimental datasets available. Therefore, as a conservative criterion, it was assumed that the error was uniformly distributed around the fitted model, and uncertainty factors were determined to cover the whole experimental dataset. In this way, the ranges of the uncertainty factors obtained were 1 ± 0.025 and 1 ± 0.020 for the liquid and vapour enthalpies, respectively.

Tray efficiency uncertainty was characterised using the assessment of the tray model performed (Syeda et al., 2007). The authors claim that its model predicts point efficiency data within $\pm 10\%$ for the sets studied. This value can be used as an estimation of the uncertainty range of overall tray efficiency. However, we expanded the range to $\pm 12.5\%$ to account for bias due to the correlations that relate point and overall tray efficiency and for other possible uncertainty effects such as feed impurities. The range for the uncertainty factor used to modify the value of tray efficiency estimated by the model was [0.875, 1.125].

Table 3 summarises the model uncertainty factors with the ranges for their respective uniform distributions. It also indicates the labels used in the various graphic analyses.

Table 3. Uncertainty ranges obtained for the distillation of methanol–water and feed variabilities considered in the uncertainty and sensitivity study.

<i>Uncertainty factor description</i>	<i>Label</i>	<i>Uncertainty ranges</i>
Perturbation for methanol activity coefficient	A1	[-0.28, 0.28]
Perturbation for water activity coefficient	A2	[-0.45, 0.47]
Uncertainty factor for liquid enthalpy	HL	1 ± 0.025
Uncertainty factor for vapor enthalpy	HV	1 ± 0.020
Uncertainty factor for overall tray efficiency	E	1 ± 0.125
Variability of feed flow	F	1 ± 0.03, 1 ± 0.06, 1 ± 0.09
Variability of feed methanol fraction	zF	1 ± 0.03, 1 ± 0.06, 1 ± 0.09
Variability of feed enthalpy	hF	1 ± 0.03, 1 ± 0.06, 1 ± 0.09

3.3 Morris analysis for towers operating with specified product composition

For the three tower configurations selected, Figure 4 shows the Morris analysis of normalised reflux ratio and reboiler heat duty ($R^* = R/R_{det}$ and $Q_B^* = Q_B/Q_{Bdet}$) (see Appendix A). For each uncertainty factor defined in Table 3, the obtained values of standard deviation σ were plotted versus the modified mean μ^* . In these figures, the line $\sigma = \mu^*$ is represented to easily identify factors for which $\sigma > \mu^*$, indicating that they show non-linear interaction with other uncertainty factors. The importance rank of each factor is related to its μ^* value. According to this, the analysis of the reflux ratio response R^* showed that the uncertainties of efficiency (E) and activity model (A1, A2) were always the most important while the importance of the enthalpy uncertainty factors was negligible. The μ^* value of the feed uncertainty factors (F, hF, zF) increased with the level of feed variability but was not able to achieve the value of the efficiency and activity model factors in the range of feed variability studied.

In the case of the reboiler heat duty response Q_B^* , the μ^* value of the feed uncertainties was more influenced by the level of feed variability and became as important as that of the model uncertainties (E, A1, A2) for a variability level of $\pm 6\%$ in tower configurations T1 and T3 and $\pm 9\%$ for tower configuration T6. This implies a higher impact of the feed variability on the setting of the operation point for the reboiler heat duty, especially when the tower has a higher number of stages. For this variable, the importance of the enthalpy uncertainty factors was negligible too.

For both responses and configurations T1 and T3, the coordinate σ was always smaller than μ^* , indicating that the effects of the factors were predominantly linear at low interaction contributions. However, for tower configuration T5 the ratio σ/μ^* was higher than 1 for the uncertainty factors associated with feed variability, while factors A2 and E reached σ/μ^* ratios near to or higher than 1. This means that as the number of trays decreases, there is higher interaction between the feed uncertainty and the model-related factors.

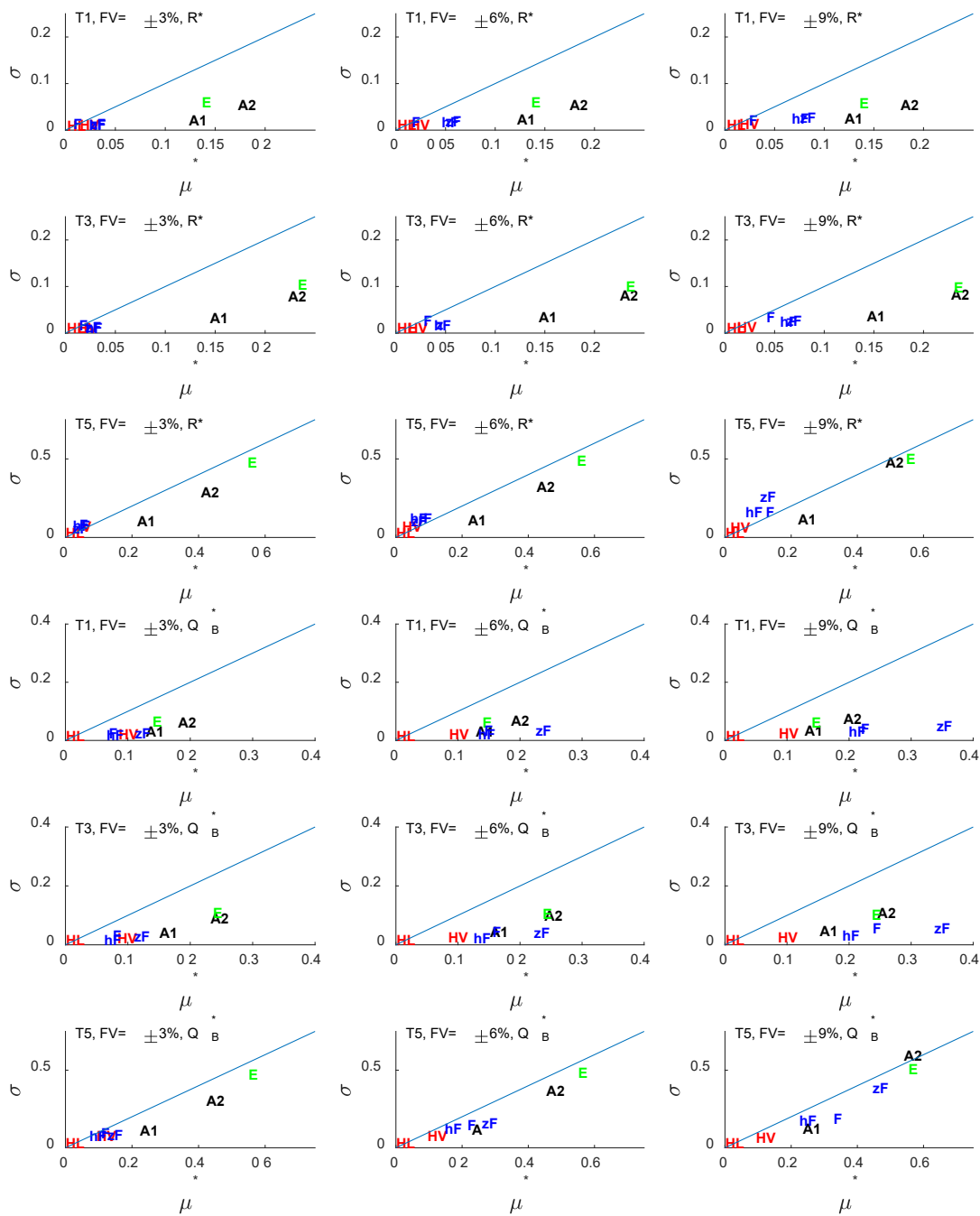


Figure 4. Morris analysis of normalized reflux ratio (R^*) and reboiler heat duty (Q_B^*) for tower configurations T1, T3, and T5 operating at specified product compositions ($x_D = 0.95, x_W = 0.05$) and three feed variability levels (FV).

The Morris analysis for these responses showed that the uncertainty factors F and zF were the only relevant ones in the uncertainty of the product flows and that their effect is independent of tower configuration (Supplemental material, Figures S1 and S2). The reason is that if product composition is specified, the product flows are directly related to the flow and composition of the feed by mass balances.

3.4 Morris analysis for towers operating at fixed reflux and reboiler heat duty

For this operation mode, the results were rather independent of the tower configuration (Supplemental material, Figures S3–S6); therefore, in this section only the results for configuration T3 are shown (Figure 5) as an intermediate case between configurations T1 and T5. According to (Pilavachi et al., 2000) the high driving-force of methanol-water separation implies that the sensitivity of the design to change in the property values is lower than other more difficult separations.

Figure 5 shows the Morris analysis of the methanol fractions on the top product and bottom product for tower configuration T3 at three levels of feed variability. According to the value of μ^* , the model uncertainty factors A1, A2 and E only were more important for distillate composition at low feed variability. For the distillate and bottom composition, the most influential factor related with feed variability was the uncertainty of the feed composition. There was also now a higher uncertainty effect of the vapour enthalpy, which could have an importance rank equal to, or even greater than model uncertainty factors at feed variability greater than 3%. In general the values of the ratio σ/μ^* were higher for the distillate composition than for the bottom composition what means a higher non-linear interaction between factors. The reason may lie in the higher number of stages in the rectification section.

Figure 5 also shows the Morris analysis of the top product and bottom product flows for tower configuration T3 at three levels of feed variability. The results can be compared with the previous case in which the methanol product fractions were fixed. Now, the model parameter factors A1, A2, E had also negligible effect on the variability of the product flows. However, besides the feed flow and composition variability, the enthalpy variability of the feed and the uncertainty of the enthalpy model were also important. In the previous case, the control needed to fix the product compositions compensates any possible uncertainty of the thermal-related factors while in the present case this compensation does not occur.

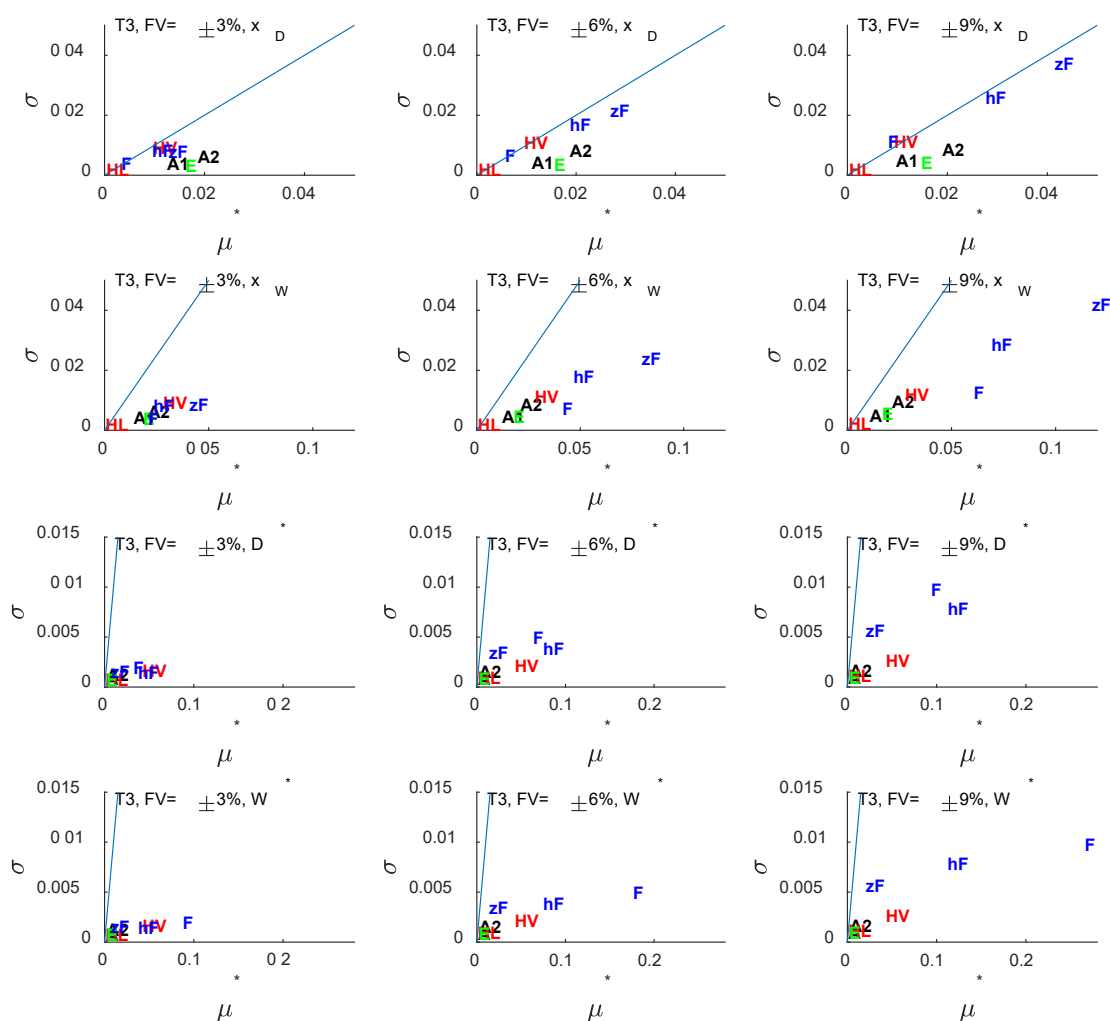


Figure 5. Morris analysis of methanol fractions on top product (x_D) and bottom product (x_W) for tower configuration T3 operating at reference reflux ratio and reboiler heat duty for three feed variability levels (FV).

3.5 Sobol analysis for a tower operating at specified product composition

The Sobol sensitivity analysis was performed for the tower configuration T3 at a feed variability level of $\pm 6\%$. Table 4 shows the results for the reflux ratio and reboiler heat duty responses which include the estimated values of the first and total Sobol indices for each factor and their respective confidence intervals. The input factors with values of the total Sobol sensitivity index greater than 0.1 were considered significant. The analysis repeated discarding the less relevant factors according to the previous Morris analysis showed similar values of the Sobol indices for the relevant factors with a smaller number of evaluations (Supplemental material, Table S1).

The analysis of the reflux ratio response yielded that the most relevant uncertainty parameters were those associated to the equilibrium model (A1, A2) and tray efficiency (E), as they had first indices and total indices much greater than those of the remaining factors. According to the total indices, the three parameters accounted for 98% of the total variability of the response. Besides, the values of the first and total Sobol

indices were very similar, which is indicative that the interaction between factors could be considered negligible. The importance rank of the input variables is consistent with the previous Morris analysis. The analysis of the reboiler heat duty revealed that the model uncertainty factors (A1, A2) and the efficiency-related one (E) and the uncertainty factor related to feed composition (zF) were relevant at the level of input variability studied. Besides, for these factors, the first Sobol indices were significantly smaller than their corresponding total Sobol indices, indicating interaction with other inputs. This interaction was not captured by the Morris screening, as low values of the σ/μ^* ratio were obtained for these factors. For the product flows, the Sobol analysis corroborated the results of the Morris analysis, as the uncertainties in F and zF were the only influential ones (Supplemental material, Table S2). All in all, the results indicate that the uncertainties in equilibrium and efficiency are critical for the control of the reflux. For the reboiler heat duty, besides these variables, the variability of the feed composition must also be taken into account.

Table 4. Sobol analysis of normalised reflux ratio and reboiler heat duty at specified product composition for tower configuration T3 and feed variability of $\pm 6\%$ ($n = 1000$, $n_{boot} = 1000$)

Variable	Factor	First index			Total index		
		orig.	min. c.i.	max. c.i.	orig.	min. c.i.	max. c.i.
Normalised reflux ratio, R^*	A1	<u>0.1595</u>	0.0657	0.2447	<u>0.1692</u>	0.1504	0.1905
	A2	<u>0.4425</u>	0.3808	0.5062	<u>0.4487</u>	0.4054	0.5045
	HL	-0.0302	-0.1367	0.0715	0.0000	0.0000	0.0000
	HV	-0.0291	-0.1335	0.0733	0.0010	0.0009	0.0011
	E	<u>0.3293</u>	0.2438	0.3953	<u>0.3600</u>	0.3238	0.3976
	F	-0.0129	-0.1192	0.0936	0.0071	0.0063	0.0082
	zF	-0.0281	-0.1401	0.0768	0.0120	0.0107	0.0136
	hF	-0.0198	-0.1243	0.0862	0.0112	0.0099	0.0124
Normalised reboiler heat duty, Q_B^*	A1	0.0231	-0.0690	0.1258	<u>0.1078</u>	0.0947	0.1180
	A2	<u>0.2252</u>	0.1621	0.3287	<u>0.2889</u>	0.2589	0.3205
	HL	-0.1134	-0.2083	-0.0141	0.0000	0.0000	0.0000
	HV	-0.0828	-0.1688	0.0106	0.0283	0.0243	0.0318
	E	<u>0.1155</u>	0.0440	0.1916	<u>0.2340</u>	0.2052	0.2530
	F	0.0176	-0.0697	0.1014	0.0979	0.0879	0.1078
	zF	<u>0.1452</u>	0.0590	0.2417	<u>0.2101</u>	0.1794	0.2328
	hF	-0.0437	-0.1434	0.0514	0.0614	0.0539	0.0675

3.6 Sobol analysis for a tower operating at fixed reflux and reboiler heat duty

The Sobol sensitivity analysis was performed for the tower configuration T3 at a feed variability level of $\pm 6\%$. Table 5 shows the results for the distillate composition (x_D) and bottom composition (x_B) which include the estimated values of the first and total Sobol indices for each factor and their respective

confidence intervals. The input factors with values of the total Sobol sensitivity index greater than 0.1 were considered significant.

For both product compositions (x_D and x_W), the most relevant factors were the uncertainty of the feed composition (zF) and the uncertainty of the feed enthalpy. There was also a small influence of the equilibrium uncertainty factor A2 in the case of the x_D response, and of the feed flow uncertainty (F) in the case of the x_W response. The results obtained were quite different from those of the previously discussed operational mode. In this case, the contribution of the input variability was much greater than the equilibrium model and efficiency uncertainties. The sums of the total Sobol indices of the feed uncertainty factors were 0.71 and 0.85 for the x_D and x_W responses, respectively, the contribution of the zF factor being the most important. On the other hand, the sum of the total Sobol indices of the equilibrium model only accounted for 0.19 for x_D and 0.05 for x_W . It is also remarkable that the effect of the efficiency uncertainty was very low.

For this operational mode, the product flow variability was almost fully determined by the variability of the feed flow variability and feed enthalpy variability with a non-negligible contribution from vapour enthalpy uncertainty in the case of the top product (Supplemental material, Table S3).

For the case studied, the greater importance of the input variability with respect to the model uncertainties (equilibrium and efficiency) can be explained by the non-existence of control actions to counteract the effects of input variability. In this case, there are no modifications of heat flows, and the effect of feed enthalpy becomes relevant. For the controlled tower to obtain a specified composition, the reflux and the reboiler can be set to suitable values, and the uncertainty in the model variables become more important as they determine the exactitude of the correct changes.

Comparing the information obtained with that provided by the Morris method, it can be said that the importance rank of the factors was quite similar. However, the Morris method indicated high values of the σ/μ^* ratio for the factors zF and hF, while the Sobol analysis threw up similar values of the respective first and total Sobol indices, which is indicative of a low interaction with other input variables.

Table 5. Sobol analysis of distillate and bottom composition at given operating conditions for tower configuration T3 and feed variability of $\pm 6\%$ (n = 1000, nboot = 100)

Variable	Factor	First index			Total index		
		orig.	min. c.i.	max. c.i.	orig.	min. c.i.	max. c.i.
Distillate methanol fraction	A1	0.0782	-0.0192	0.1847	0.0612	0.0521	0.0691
	A2	<u>0.1347</u>	0.0531	0.2250	<u>0.1311</u>	0.1105	0.1494
	HL	0.0260	-0.0585	0.1307	0.0001	0.0000	0.0001
	HV	0.0928	0.0113	0.2158	0.0598	0.0509	0.0670
	E	<u>0.1172</u>	0.0275	0.2136	0.0920	0.0728	0.1014
	F	0.0612	-0.0161	0.1917	0.0731	0.0617	0.0837
	zF	<u>0.4153</u>	0.3526	0.5103	<u>0.4423</u>	0.3863	0.5048
	hF	<u>0.1911</u>	0.1068	0.2935	<u>0.1987</u>	0.1583	0.2219
Bottom methanol fraction	A1	-0.0239	-0.0940	0.0679	0.0176	0.0156	0.0196
	A2	0.0032	-0.0627	0.0964	0.0368	0.0323	0.0414
	HL	-0.0533	-0.1186	0.0271	0.0000	0.0000	0.0000

HV	0.0136	-0.0559	0.0892	0.0672	0.0584	0.0762
E	-0.0135	-0.0820	0.0613	0.0264	0.0235	0.0285
F	<u>0.1089</u>	0.0447	0.1811	<u>0.1267</u>	0.1125	0.1402
zF	<u>0.5169</u>	0.4769	0.5678	<u>0.5324</u>	0.4811	0.5801
hF	<u>0.1426</u>	0.0762	0.2106	<u>0.1889</u>	0.1707	0.2078

3.7 Uncertainty analysis

For the case of specified product compositions, the uncertainty limits of the normalised reflux response were not affected by the input feed variability, and the uncertainty limits of the normalised heat duty slightly increased with input feed variability (Figure 6). However, for both responses, there was an important effect of the tower configuration: the smaller the tower size, the greater the width of the uncertainty band. The reason is that for a tower with fewer trays, the changes in the operating point must be greater to counteract the deviation of the input feed with respect to their nominal values. Because of the direct relation between the uncertainty of F and zF previously mentioned, the uncertainty band for the flow products increases from zero as the feed variability is increased, the results being independent of tower configuration.

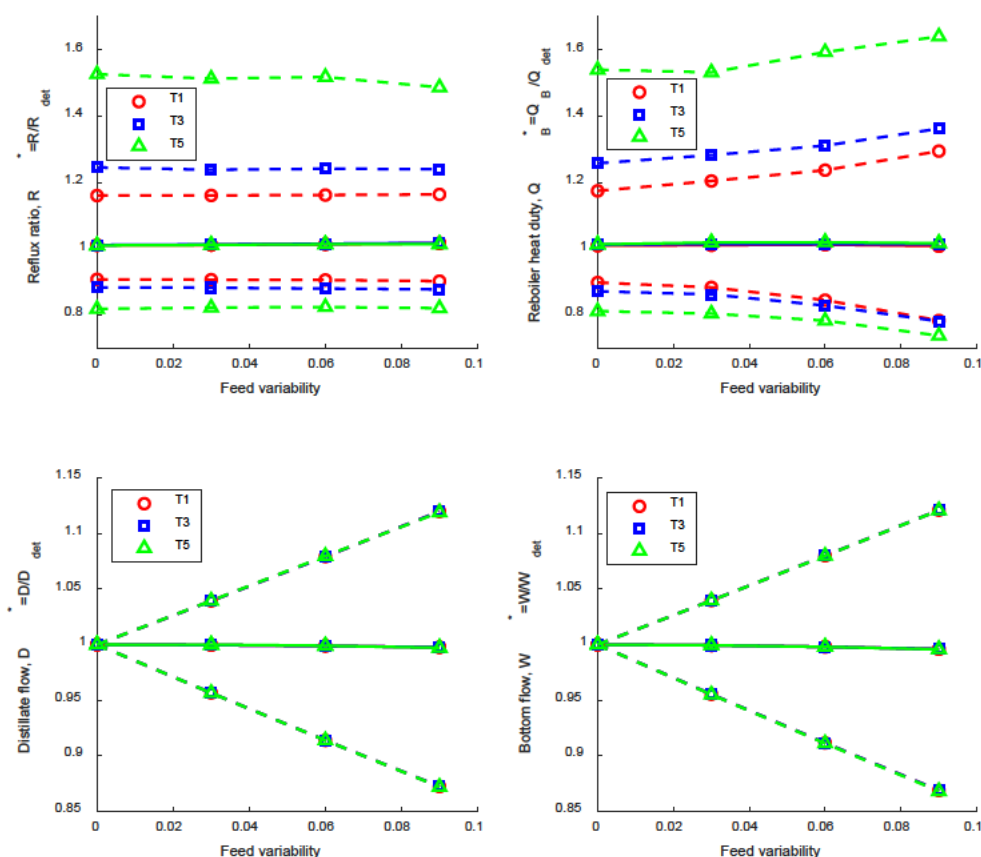


Figure 6. Effect of feed variability on uncertainty limits (dash lines) and median (full lines) of normalised responses at specified product composition for tower configurations T1, T3 and T5.

In the case of fixed operation, the uncertainty band for the response variables x_D and x_W increased with input variability and there was low influence of the tower configuration (Figure 7). As the distillation and bottom fractions are bounded variables, the increase in the distillation upper limit and the decrease in the bottom lower limit are also bounded and vary slightly with input feed variability. However, the uncertainty in lower limit for the distillate fraction was approximately 0.94 times its nominal value and the upper limit of the bottom fraction 2.7 times its nominal value. The higher uncertainty in the bottom composition is due to the low number of stages in the stripping zone, which makes the bottom composition more sensitive to deviations in input feed from the reference value. As in the case of specified product composition, the uncertainty in the product flows increased with the input feed variability, but the width of the uncertainty band was not zero for zero input feed variability because both sets of variables are related by the model, and consequently by its associated uncertainties.

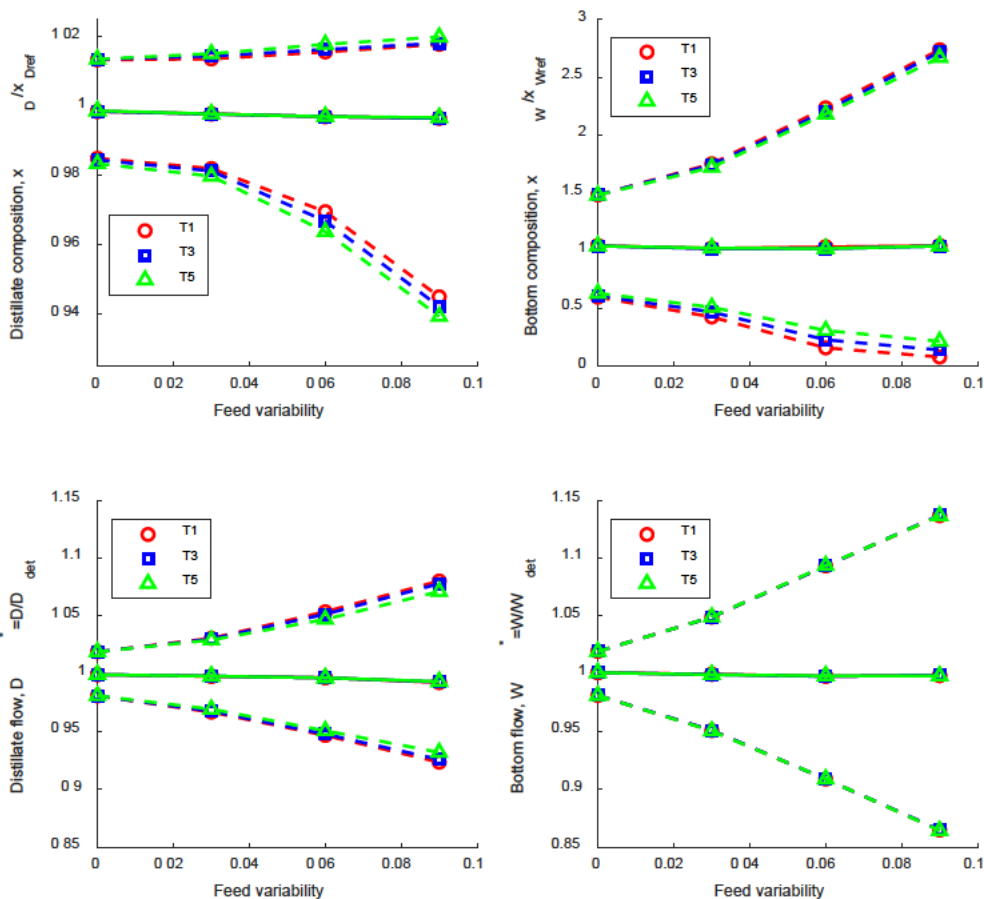


Figure 7. Effect of feed variability on uncertainty limits (dash lines) and median (full lines) of normalised responses at specified operation conditions for tower configurations T1, T3 and T5.

Note: This is the pre-print version previous to the reviewing process of:
Gozálvez-Zafilla, J.M., García-Díaz, J.C., Santafé-Moros, A., 2021. Uncertainty quantification and global sensitivity analysis of continuous distillation considering the interaction of parameter uncertainty with feed variability. Chem. Eng. Sci. 235, 116509. <https://doi.org/10.1016/j.ces.2021.116509>
<https://linkinghub.elsevier.com/retrieve/pii/S0009250921000749>

4 Conclusions

Uncertainty and sensitivity analyses were applied to a continuous distillation code to study the interaction of parameter uncertainty with feed and operation variability for a specific case of methanol–water distillation. Two operational modes, fixed product composition and fixed operation conditions, were studied for three selected tower configurations corresponding to different reflux-to-minimum-reflux ratios. Depending on the operational mode, the study focused respectively on the analysis of reflux ratio and reboiler heat duty or the methanol composition of the product streams.

The model parameter uncertainty was expressed by using uniform distributions of the parameter in appropriate ranges to cover the spread of experimental data. The analysis of the experimental VLE data revealed significant differences between the available data sets used. In this case, two perturbation parameters were associated with the NRTL activity coefficient model. The range of efficiency-related uncertainty was greater than $\pm 10\%$ in spite of having used an advanced efficiency model. Feed variability was modelled using uniform distributions with ranges of different width centred on the reference values of the feed variables.

The sensitivity study was carried out in two phases. In the first phase, the Morris screening method was applied to the three tower configurations selected at three feed variability levels ($\pm 3\%$, $\pm 6\%$, $\pm 9\%$). The screening phase provided valuable information for the ranking of the input variables by importance according to their influence on the output of the computational model. This analysis revealed the high importance of the VLE and efficiency-related factors and showed greater importance of the feed factors as the feed variability increased. However, depending on the operational mode studied, the relative importance of feed- and model-related parameters was different. The Morris analysis also indicated that, for most situations, the effects of the factors studied were predominantly linear and very similar for the different tower configurations. In the second phase of the sensitivity study, the Sobol variance decomposition method was applied to the tower configuration with central reflux-to-minimum reflux ratio at a feed variability level of $\pm 6\%$. The values of the Sobol indices obtained were in agreement with the importance rank of the factors obtained by the Morris analysis. However, the Sobol analysis was able to determine with more precision than the Morris analysis the existence of non-linear effects and interactions by comparing the value of the first and total Sobol indices. The Morris method is much less computer-intensive than the Sobol indices calculation and can be suitable when we are interested only in the rank importance of the input factors. It does not achieve a precise quantification of the interaction of the input variables, which the Sobol method does.

The uncertainty analysis revealed different behaviour for the two operating modes studied. For the study at specified product composition the uncertainty limits of the reflux and reboiler heat duty response were slightly affected by the input feed variability, but there were important differences according the tower configuration. Conversely, at fixed operation, there was an important effect of input variability and low influence of tower configuration.

The importance of the effects observed justifies the necessity for uncertainty studies for the robust design of distillation towers and sensitivity studies to understand the different impacts of the uncertainty sources on the model response.

Appendix A

A.1 Morris One-at-a-Time (MOAT) screening method

In the MOAT method (Saltelli et al., 2004), each input factor to the computational model is divided equally into p levels. The space of inputs is discretised in an n -dimensional grid with p levels by input. An elementary effect (d_i) corresponding to an input X_i is determined by Eq. A1:

$$d_i(x) = \frac{y(x + \Delta e_i) - y(x)}{\Delta} \quad (\text{A1})$$

where e_i is a vector of canonical base, and Δ is the step used to evaluate the computational model and find the elementary effect given by Eq. A2:

$$\Delta = \frac{p}{2(p-1)} \quad (\text{A2})$$

For each input of the computational model a distribution of elemental effects on the response variable is formed. After generating r samples (number of One-at-a-Time designs) of this distribution, the mean value μ_i , the modified mean value μ_i^* , and the standard deviation σ_i are obtained according to Eqs. A3–A5:

- Mean:

$$\mu_i = \frac{1}{r} \sum_{j=1}^r d_i^{(j)} \quad (\text{A3})$$

- Modified mean:

$$\mu_i^* = \frac{1}{r} \sum_{j=1}^r |d_i^{(j)}| \quad (\text{A4})$$

- Standard deviation:

$$\sigma_i = \sqrt{\frac{1}{r} \sum_{j=1}^r (d_i^{(j)} - \mu_i)^2} \quad (\text{A5})$$

The above parameters can be interpreted as follows. The criterion μ_i^* is a good indicator by which to classify input variables by order of importance, despite the fact that information about the sign of the elementary effects is lost. Moreover, the standard deviation of the elementary effects σ_i is a relevant indicator of non-linearity in input parameters of the model or interactions with other parameters involved in the model. By plotting both statistical indicators, the Morris method identifies the inputs that can be considered to have an effect, according to:

1. Negligible effect (low μ^* , low σ).
2. Linear and additive effect (high μ^* , low σ).
3. Non-linear or involved in interactions with other input parameters (high σ).

The total number of computational model evaluations performed (model calls) is $N = r \cdot (n+1)$, where n is the number of input factors. Saltelli et al. (Saltelli, 2002) recommend using the following values for the method parameters: $r = 4$ to 10 samples and $p = 4$ levels.

A.2 Sensitivity analysis: Variance-based decomposition. Sobol's indices

The different inputs of the model input random vector $X = (X_1, X_2, \dots, X_n) \in \mathbb{R}^n$ are assumed to be uncorrelated and uniformly distributed on the unit hypercube $[0, 1]^n$. The output model $Y = f(X)$ is a random variable, $Y \in \mathbb{R}$. According to (Sobol, 1993), the output can be decomposed into summands of increasing dimensionality:

$$Y = f(X) = f_0 + \sum_{i=1}^n f_i(X_i) + \sum_{i<j}^n f_{ij}(X_i, X_j) + \dots + f_{12\dots d} \quad (\text{A6})$$

The objective of the variance decomposition is to express the variance of the output of the computation model $f(X)$ as a finite sum of terms of increasing order (Eq. A7). Each of these terms represents the contribution V_i of an input variable X_i to the output variance (first-order terms) or the variance V_{ij} due to interactions of several variables (higher-order terms). In the case of uncorrelated variables, this decomposition is unique (Sobol, 1993).

$$\text{Var}(Y) = \sum_{i=1}^n V_i + \sum_{i<j}^n V_{ij} + \dots + V_{1,2,\dots,d} \quad (\text{A7})$$

where:

$$V_i = \text{Var}_{X_i}[E_{X_{\sim i}}(Y/X_i)] \quad (\text{A8})$$

$$V_{i,j} = \text{Var}_{X_{ij}}[E_{X_{\sim ij}}(Y/X_{ij})] \quad (\text{A9})$$

$$X_{\sim i} = (X_1, \dots, X_{i-1}, X_{i+1}, \dots, X_n) \quad (\text{A10})$$

The Sobol sensitivity indices are defined as the partial variances normalised by the output variance. The first-order indices S_i indicate the expected reduction in the variance if the input X_i is set, without considering the interactions with other inputs. The total sensitivity indices S_{T_i} indicate the reduction of the variance that would occur if all entries, except X_i , were fixed. S_{T_i} incorporates estimates of all interactions with other inputs. Considering Eqs. A7–A10 the first-order and total Sobol indices are defined as follows:

$$S_i = \frac{V_i}{\text{Var}(Y)} \quad (\text{A11})$$

$$S_{T_i} = \frac{E_{X_{\sim i}}[\text{Var}_{X_i}(Y/X_{\sim i})]}{\text{Var}(Y)} = 1 - \frac{\text{Var}_{X_{\sim i}}[E_{X_i}(Y/X_{\sim i})]}{\text{Var}(Y)} \quad (\text{A12})$$

Some considerations should be commented on the values of the Sobol indices. First of all, it is fulfilled that $0 \leq S_i \leq S_{T_i} \leq 1$, $\sum_{i=1}^n S_i \leq 1$ and $\sum_{i=1}^n S_{T_i} \geq 1$.

Other considerations are shown below

- If $S_i = S_{T_i}$, there are no interactions between X_i and the other inputs.
- If $S_i = 0$, $f(\mathbf{X})$ does not depend on X_i , but X_i can have interactions with other inputs.
- If $S_i = 1$, $f(\mathbf{X})$ depends only on X_i .
- If $S_{T_i} \ll 1$, $f(\mathbf{X})$ does not depend on X_i and X_i can be set to a constant value.

Besides, the higher-order effects due to parameter interactions ($S_{T_i} - S_i$) are important and cannot be ignored even if S_i is small.

Sensitivity indices are computed using Monte Carlo sampling. A total number of N code runs are performed, varying simultaneously the values of all uncertain input parameters according to their distribution. The computational cost of this method is usually very high in terms of the number of calls to the computational model. The number of evaluations N of the model is usually of the order of 10^4 to obtain an adequate precision in the estimation of the Sobol sensitivity indices. The number of model calls is $N = N^* \cdot (n + 2)$, where N^* is the size of the initial Monte Carlo sample and n is the number of inputs. Estimators for S_i and S_{T_i} have been reviewed by (Saltelli et al., 2010b) and (Iooss and Lemaître, 2015).

List of Variables

A1	uncertainty factor for methanol activity coefficient
A2	uncertainty factor for water activity coefficient
D	distillate product flow, kmol/h
D^*	normalised distillate product flow, $D^* = D/D_{det}$
E	uncertainty factor for efficiency
E_{MV}	Murphree's vapour tray efficiency
F	feed flow (in case of single feed), kmol/h
F_n	feed flow entering to stage n , kmol/h
f_v	vapour fraction in the feed
FV	feed variability defined as percentage of variation with respect to the deterministic value
G_{12}	term of the NRTL model
G_{21}	term of the NRTL model
h_{AD}	enthalpy coordinate of distillate pole, kJ/kmol
h_{AW}	enthalpy coordinate of bottom pole, kJ/kmol
h_F	feed enthalpy (in case of single feed), kJ/kmol
h_G	enthalpy of vapour stream, kJ/kmol
h_L	enthalpy of liquid stream, kJ/kmol
L_n	liquid flow exiting from stage n , kmol/h
N	number of stages of the distillation tower

N	number of Monte Carlo runs
N_F	feed stage position
n	number of samples in Morris analysis
n_{boot}	number of bootstrap replicates in Morris analysis
p	number of levels in Morris analysis
P_i	partial pressure of component i , Pa
P_t	total pressure, Pa
$P_{vap,i}$	vapour pressure of component i , Pa
Q_B	reboiler heat duty, kJ/h
Q_B^*	normalised reboiler heat duty $Q_B^* = Q_B/Q_{B,det}$
$Q_{B,det}$	deterministic reboiler heat duty, kJ/h
Q_C	deterministic reboiler heat duty, kJ/h
q_n	external heat flux entering to stage n , kJ/h
r	number of Morris samples
R	reflux ratio
R^*	normalised reflux ratio $R^* = R/R_{det}$
R_{det}	deterministic reflux ratio
R_g	gas perfect constant, $8.314 \text{ J}\cdot\text{mol}^{-1}\cdot\text{K}^{-1}$
s_j	generic NRTL parameter
S_i	first Sobol index of factor i
S_{Ti}	total Sobol index of factor i
T	temperature, K
T_n	temperature in stage n , K
V_n	vapour flow exiting from stage n , kmol/h
W	bottom product flow, kmol/h
W^*	normalised bottom product flow, $W^*=W/W_{det}$
x	vector of mole fractions of key component in liquid streams
$x^{<k>}$	vector of mole fractions of key component in liquid streams in k iterations
x_D	methanol fraction in the top product
x_F	methanol fraction in the feed
x_{Dref}	methanol fraction specification in the top product for the reference case
$x_{n,i}$	molar fraction of component i in stage n
x_W	methanol fraction in the bottom product
x_{Dref}	methanol fraction specification in the bottom product for the reference case
X_i	generic input variable
X_i^o	reference value of generic input variable
Y	generic model response
y_n	average mole fraction of light key component in the vapour leaving stage n
y_{n+1}	average mole fraction of light key component in the vapour leaving stage n

y_n^* equilibrium mole fraction of light key component in the vapour leaving stage n
 z_F methanol fraction in the feed

Greek letters

α NRTL parameter
 δ_i perturbation parameter
 γ_j liquid phase activity coefficients of component j
 γ^p perturbed value of activity coefficient
 γ^m model deterministic value of activity coefficient
 Δg_{12} NRTL parameter
 Δg_{21} NRTL parameter
 Φ error function for model parameters
 σ_i Morris standard deviation of factor i
 τ_{12} NRTL term
 τ_{21} NRTL term
 μ Morris mean of factor i
 μ^* Morris modified mean of factor i

References

- Abello, L., 1973. Enthalpies d'excès des systèmes binaires constitués d'hydrocarbures benzéniques et du chloroforme ou du méthylchloroforme. *J. Chim. Phys.* 70, 1355–1359.
- Abolpour, B., Abolpour, R., Shamseddini, A., Kamyabi, S., Hamzehee, F., 2013. Optimization of the reflux ratio for methanol–water stage distillation column. *Res. Chem. Intermed.* 39, 681–692. <https://doi.org/10.1007/s11164-012-0589-7>
- Aneesh, V., Antony, R., Paramasivan, G., Selvaraju, N., 2016. Distillation technology and need of simultaneous design and control: A review. *Chem. Eng. Process. Process Intensif.* <https://doi.org/10.1016/j.cep.2016.03.016>
- Bassat, J.-M., Petitjean, P., Fouletier, J., Lalanne, C., Caboche, C., Mauvy, F., Grenier J-C, 2005. Oxygen isotopic exchange: A useful tool for characterizing oxygen conducting oxides. *Appl. Catal. A.* <https://doi.org/10.1016/j.apcata.2005.04.054>
- Benjamin, L., Benson, G.C., 1963. A deuterium isotope effect on the excess enthalpy of methanol—water solutions 1. *J. Phys. Chem.* 67, 858–861. <https://doi.org/10.1021/j100798a034>
- Biddulph, M.W., Kalbassi, M.A., 1988. Distillation efficiencies for methanol/1-propanol/water. *Ind. Eng. Chem. Res.* 27, 2127–2135. <https://doi.org/10.1021/ie00083a029>
- Buddenberg, J.W., Wilke, C.R., 1949. Calculation of gas mixture viscosities. *Ind. Eng. Chem.* 41, 1345–1347. <https://doi.org/10.1021/ie50475a011>
- Campolongo, F., Cariboni, J., Saltelli, A., 2007. An effective screening design for sensitivity analysis of large models. *Environ. Model. Softw.* 22, 1509–1518. <https://doi.org/10.1016/J.ENVSOF.2006.10.004>
- CHERIC (Chemical Engineering and Materials Research Information Center), n.d. KDB (Korea Thermophysical Properties Data Bank): Binary Vapor-Liquid Equilibrium Data [WWW Document]. URL www.cheric.org/research/kdb/hcvle/hcvle.php (accessed 4.10.18).
- Chunxi, L., Wenchuan, W., Zihao, W., 2000. A surface tension model for liquid mixtures based on the Wilson equation. *Fluid Phase Equilib.* 175, 185–196. [https://doi.org/10.1016/S0378-3812\(00\)00447-7](https://doi.org/10.1016/S0378-3812(00)00447-7)
- Couper, J.R., Penney, W.R., Fair, J.R., Walas, S.M.B.T. (Eds.), 2010. Distillation and absorption, in: *Chemical Process Equipment*. Gulf Professional Publishing, Boston, pp. 395–480. <https://doi.org/https://doi.org/10.1016/B978-0-12-372506-6.00021-6>
- Dalager, P., 1969. Vapor-liquid equilibriums of binary systems of water with methanol and ethanol at extreme dilution of the alcohols. *J. Chem. Eng. Data* 14, 298–301. <https://doi.org/10.1021/je60042a022>
- DDBST, n.d. Dortmund Data Bank: Metanol-water vapor-liquid equilibrium data [WWW Document]. DDB Explor. Ed. URL www.ddbst.com (accessed 4.10.18).
- DDBST GmbH, n.d. Dortmund Data Bank - PPC Pure component properties [WWW Document]. URL <http://www.ddbst.com/ddb-ppc.html> (accessed 4.4.18).
- Dunlop, J.G., 1948. Vapor-Liquid Equilibrium Data. Brooklyn Polytechnic Institute, New York.

- Enagandula, S., Riggs, J.B., 2006. Distillation control configuration selection based on product variability prediction. *Control Eng. Pract.* 14, 743–755. <https://doi.org/10.1016/j.conengprac.2005.03.011>
- Fuller, E.N., Schettler, P.D., Giddings, J.C., 1966. New method for prediction of binary gas-phase diffusion coefficients. *Ind. Eng. Chem.* 58, 18–27. <https://doi.org/10.1021/ie50677a007>
- Garcia, J.A., Fair, J.R., 2000. A fundamental model for the prediction of distillation sieve tray efficiency. 1. Database development. *Ind. Eng. Chem. Res.* 39, 1809–1817. <https://doi.org/10.1021/ie990875q>
- Garcia, J Antonio, Fair, J.R., 2000. A Fundamental Model for the Prediction of Distillation Sieve Tray Efficiency. 2. Model Development and Validation. *Ind. Eng. Chem. Res.* 39, 1818–1825. <https://doi.org/10.1021/ie0000966>
- Gau, C.-Y., Brennecke, J.F., Stadtherr, M.A., 2000. Reliable nonlinear parameter estimation in VLE modeling. *Fluid Phase Equilib.* 168, 1–18. [https://doi.org/10.1016/S0378-3812\(99\)00332-5](https://doi.org/10.1016/S0378-3812(99)00332-5)
- Gmehling, J., Onken, U., Behrens, D., Eckermann, R., 1977. Vapor-Liquid Equilibrium Data Collection - Aqueous-organic systems, DECHEMA Chemistry data series. Frankfurt, Germany.
- Guettari, M., Gharbi, A., 2011. A correspondence between Grunberg–Nissan constant d' and complex varieties in water/methanol mixture. *Phys. Chem. Liq.* 49, 459–469. <https://doi.org/10.1080/00319101003646546>
- Henrion, R., Möller, A., 2003. Optimization of a continuous distillation process under random inflow rate. *Comput. Math. with Appl.* 45, 247–262. [https://doi.org/10.1016/S0898-1221\(03\)80017-2](https://doi.org/10.1016/S0898-1221(03)80017-2)
- Iooss, B., Lemaître, P., 2015. A Review on Global Sensitivity Analysis Methods BT - Uncertainty Management in Simulation-Optimization of Complex Systems: Algorithms and Applications, in: Dellino, G., Meloni, C. (Eds.), . Springer US, Boston, MA, pp. 101–122. https://doi.org/10.1007/978-1-4899-7547-8_5
- Jansen, M.J.W., 1999. Analysis of variance designs for model output. *Comput. Phys. Commun.* 117, 35–43. [https://doi.org/10.1016/S0010-4655\(98\)00154-4](https://doi.org/10.1016/S0010-4655(98)00154-4)
- Katayama, T., 1962. Heats of Mixing, Liquid Heat Capacities and Enthalpy-Concentration Charts for Methanol-Water and Iso-propanol-Water Systems. *Chem. Eng.* 26, 361–372. <https://doi.org/10.1252/kakoronbunshu1953.26.361>
- Katti, A.M., Tarfulea, N.E., Hopper, C.J., Kmiotek, K.R., 2008. Prediction of Viscosity–Temperature–Composition Surfaces in a Single Expression for Methanol–Water and Acetonitrile–Water Mixtures. *J. Chem. Eng. Data* 53, 2865–2872. <https://doi.org/10.1021/jc800607j>
- Khosharay, S., Tourang, S., Tajfar, F., 2017. Modeling surface tension and interface of (water+methanol), (water+ethanol), (water+1-propanol), and (water+MEG) mixtures. *Fluid Phase Equilib.* 454, 99–110. <https://doi.org/10.1016/J.FLUID.2017.09.017>
- Kubota, H., Tsuda, S., Murata, M., Yamamoto, T., Tanaka, Y., Makita, T., 1980. Specific volume and viscosity of methanol-water mixtures under high pressure. *Rev. Phys. Chem. Japan* 49, 59–69.
- Kurihara, K., Nakamichi, M., Kojima, K., 1993. Isobaric vapor-liquid equilibria for methanol + ethanol + water and the three constituent binary systems. *J. Chem. Eng. Data* 38, 446–449. <https://doi.org/10.1021/jc00011a031>
- Lashmet, P.K., Szczepanski, S.Z., 1974. Efficiency Uncertainty and Distillation Column Overdesign

- Factors. *Ind. Eng. Chem. Process Des. Dev.* 13, 103–106. <https://doi.org/10.1021/i260050a002>
- Li, P., Wendt, M., Arellano-Garcia, H., Wozny, G., 2002. Optimal operation of distillation processes under uncertain inflows accumulated in a feed tank. *AIChE J.* 48, 1198–1211. <https://doi.org/10.1002/aic.690480608>
- Luo, N., Qian, F., Ye, Z.-C., Cheng, H., Zhong, W.-M., 2012. Estimation of Mass-Transfer Efficiency for Industrial Distillation Columns. *Ind. Eng. Chem. Res.* 51, 3023–3031. <https://doi.org/10.1021/ie2008407>
- Marczak, W., Adamczyk, N., Łęźniak, M., 2012. Viscosity of Associated Mixtures Approximated by the Grunberg-Nissan Model. *Int. J. Thermophys.* 33, 680–691. <https://doi.org/10.1007/s10765-011-1100-1>
- Mathias, P.M., 2017. Guidelines for the Analysis of Vapor–Liquid Equilibrium Data. *J. Chem. Eng. Data* 62, 2231–2233. <https://doi.org/10.1021/acs.jced.7b00582>
- Mathias, P.M., 2016. Effect of VLE uncertainties on the design of separation sequences by distillation – Study of the benzene–chloroform–acetone system. *Fluid Phase Equilib.* 408, 265–272. <https://doi.org/10.1016/J.FLUID.2015.09.004>
- Mathias, P.M., 2014. Sensitivity of Process Design to Phase Equilibrium—A New Perturbation Method Based Upon the Margules Equation. *J. Chem. Eng. Data* 59, 1006–1015. <https://doi.org/10.1021/je400748p>
- Morris, M.D., 1991. Factorial sampling plans for preliminary computational experiments. *Technometrics* 33, 161–174. <https://doi.org/10.1080/00401706.1991.10484804>
- Pilavachi, P.A., Schenk, M., Bek-Pedersen, E., Gani, R., 2000. Design and analysis of separation by distillation. Role of property models. *Chem. Eng. Res. Des.* 78, 217–230. <https://doi.org/10.1205/026387600527257>
- Puentes, C., Joulia, X., Athès, V., Esteban-Decloux, M., 2018. Review and Thermodynamic Modeling with NRTL Model of Vapor–Liquid Equilibria (VLE) of Aroma Compounds Highly Diluted in Ethanol–Water Mixtures at 101.3 kPa. *Ind. Eng. Chem. Res.* 57, 3443–3470. <https://doi.org/10.1021/acs.iecr.7b03857>
- Pujol, G., 2009. Simplex-based screening designs for estimating metamodells. *Reliab. Eng. Syst. Saf.* 94, 1156–1160. <https://doi.org/10.1016/J.RESS.2008.08.002>
- R Core Team, 2018. A Language and Environment for Statistical Computing. <https://www.r-project.org/>, Vienna, Austria.
- Resetarits, M.R., Lockett, M.J., 2003. Distillation, in: *Encyclopedia of Physical Science and Technology*. Elsevier, pp. 547–559. <https://doi.org/10.1016/B0-12-227410-5/00182-4>
- Ricardez-Sandoval, L.A., 2012. Optimal design and control of dynamic systems under uncertainty: A probabilistic approach. *Comput. Chem. Eng.* 43, 91–107. <https://doi.org/10.1016/j.compchemeng.2012.03.015>
- Saghatoleslami, N., Vatankhah, G.H., Karimi, H., Noie, S.H., 2011. Prediction of the overall sieve tray efficiency for a group of hydrocarbons, an artificial neural network approach. *J. Nat. Gas Sci. Eng.* 3, 319–325. <https://doi.org/10.1016/J.JNGSE.2011.01.002>

- Saltelli, A., 2002. Making best use of model evaluations to compute sensitivity indices. *Comput. Phys. Commun.* 145, 280–297. [https://doi.org/10.1016/S0010-4655\(02\)00280-1](https://doi.org/10.1016/S0010-4655(02)00280-1)
- Saltelli, A., Annoni, P., Azzini, I., Campolongo, F., Ratto, M., Tarantola, S., 2010a. Variance based sensitivity analysis of model output. Design and estimator for the total sensitivity index. *Comput. Phys. Commun.* 181, 259–270.
- Saltelli, A., Annoni, P., Azzini, I., Campolongo, F., Ratto, M., Tarantola, S., 2010b. Variance based sensitivity analysis of model output. Design and estimator for the total sensitivity index. *Comput. Phys. Commun.* 181, 259–270. <https://doi.org/10.1016/J.CPC.2009.09.018>
- Saltelli, A., Tarantola, S., Campolongo, F., Ratto, M., 2004. *Sensitivity analysis in practice. A guide to assessing scientific models.* Jhon Wiley & Sons.
- Sánchez, S., Ancheyta, J., McCaffrey, W.C., 2007. Comparison of Probability Distribution Functions for Fitting Distillation Curves of Petroleum. *Energy & Fuels* 21, 2955–2963. <https://doi.org/10.1021/ef070003y>
- Seader, J.D., Henley, E.J., Roper, D.K., 2011. *Separation process principles: chemical and biochemical operations*, 3rd ed. NJ John Wiley and Sons, Inc, Hoboken, NJ.
- Shahandeh, H., Jafari, M., Kasiri, N., Ivakpour, J., 2015. Economic optimization of heat pump-assisted distillation columns in methanol-water separation. *Energy* 80, 496–508. <https://doi.org/10.1016/J.ENERGY.2014.12.006>
- Sobol, I.M., 1993. Sensitivity Estimates for Nonlinear Mathematical Models. *Math. Model. Comput. Exp.* 1, 407–414.
- Soujanya, J., Anvesh Reddy, C., Satyavathi, B., Sankarshana, T., 2016. Experimental vapour–liquid equilibrium data of the quaternary system Methanol (1) + Isopropyl alcohol (2) + Water (3) + Glycerol (4) along with Isopropyl alcohol (2) + Glycerol (4) and Isopropyl alcohol (2) + Water (3) binary data at atmospheric and sub-a. *Fluid Phase Equilib.* 409, 327–333. <https://doi.org/10.1016/J.FLUID.2015.09.052>
- Soujanya, J., Satyavathi, B., Vittal Prasad, T.E., 2010. Experimental (vapour + liquid) equilibrium data of (methanol + water), (water + glycerol) and (methanol + glycerol) systems at atmospheric and sub-atmospheric pressures. *J. Chem. Thermodyn.* 42, 621–624. <https://doi.org/10.1016/J.JCT.2009.11.020>
- Syeda, S.R., Afacan, A., Chuang, K.T., 2007. A Fundamental Model for Prediction of Sieve Tray Efficiency. *Chem. Eng. Res. Des.* 85, 269–277. <https://doi.org/10.1205/CHERD06111>
- Treybal, R.E., 1980. *Mass-transfer operations*, 3th ed. Singapore.
- Ulas, S., Diwekar, U.M., Stadtherr, M.A., 2005. Uncertainties in parameter estimation and optimal control in batch distillation. *Comput. Chem. Eng.* 29, 1805–1814. <https://doi.org/10.1016/j.compchemeng.2005.03.002>
- Vazquez, G., Alvarez, E., Navaza, J.M., 1995. Surface Tension of Alcohol Water + Water from 20 to 50 .degree.C. *J. Chem. Eng. Data* 40, 611–614. <https://doi.org/10.1021/je00019a016>
- Vennavelli, A.N., Whiteley, J.R., Resetarits, M.R., 2014. Predicting valve tray efficiency. *Chem. Eng. Res. Des.* 92, 2148–2152. <https://doi.org/10.1016/J.CHERD.2014.01.022>

- Vennavelli, A.N., Whiteley, J.R., Resetarits, M.R., 2012. New Fraction Jetting Model for Distillation Sieve Tray Efficiency Prediction. *Ind. Eng. Chem. Res.* 51, 11458–11462. <https://doi.org/10.1021/ie202997t>
- Verhoeve, L., De Schepper, H., 1973. The vapour—liquid equilibria of the binary, ternary and quaternary systems formed by acetone, methanol, propan-2-ol, and water. *J. Appl. Chem. Biotechnol.* 23, 607–619. <https://doi.org/10.1002/jctb.5020230807>
- Yang, C., Ma, S., Yin, X., 2011. Organic Salt Effect of Tetramethylammonium Bicarbonate on the Vapor–Liquid Equilibrium of the Methanol–Water System. *J. Chem. Eng. Data* 56, 3747–3751. <https://doi.org/10.1021/je200341c>
- Yang, N.S., Chuang, K.T., Afacan, A., Resetarits, M.R., Binkley, M.J., 2003. Improving the Efficiency and Capacity of Methanol–Water Distillation Trays. *Ind. Eng. Chem. Res.* 42, 6601–6606. <https://doi.org/10.1021/ie030407n>
- Zhong, Y., Warren, G.L., Patel, S., 2008. Thermodynamic and Structural Properties of Methanol–Water Solutions Using Non-Additive Interaction Models. *J. Comput. Chem.* 29, 1142–1152. <https://doi.org/10.1002/jcc.20877>

Uncertainty quantification and global sensitivity analysis of continuous distillation considering the interaction of parameter uncertainty with feed and operation variability

J. M. Gozávez-Zafrilla, J. C. García-Díaz, A. Santafé-Moros

Supplemental material

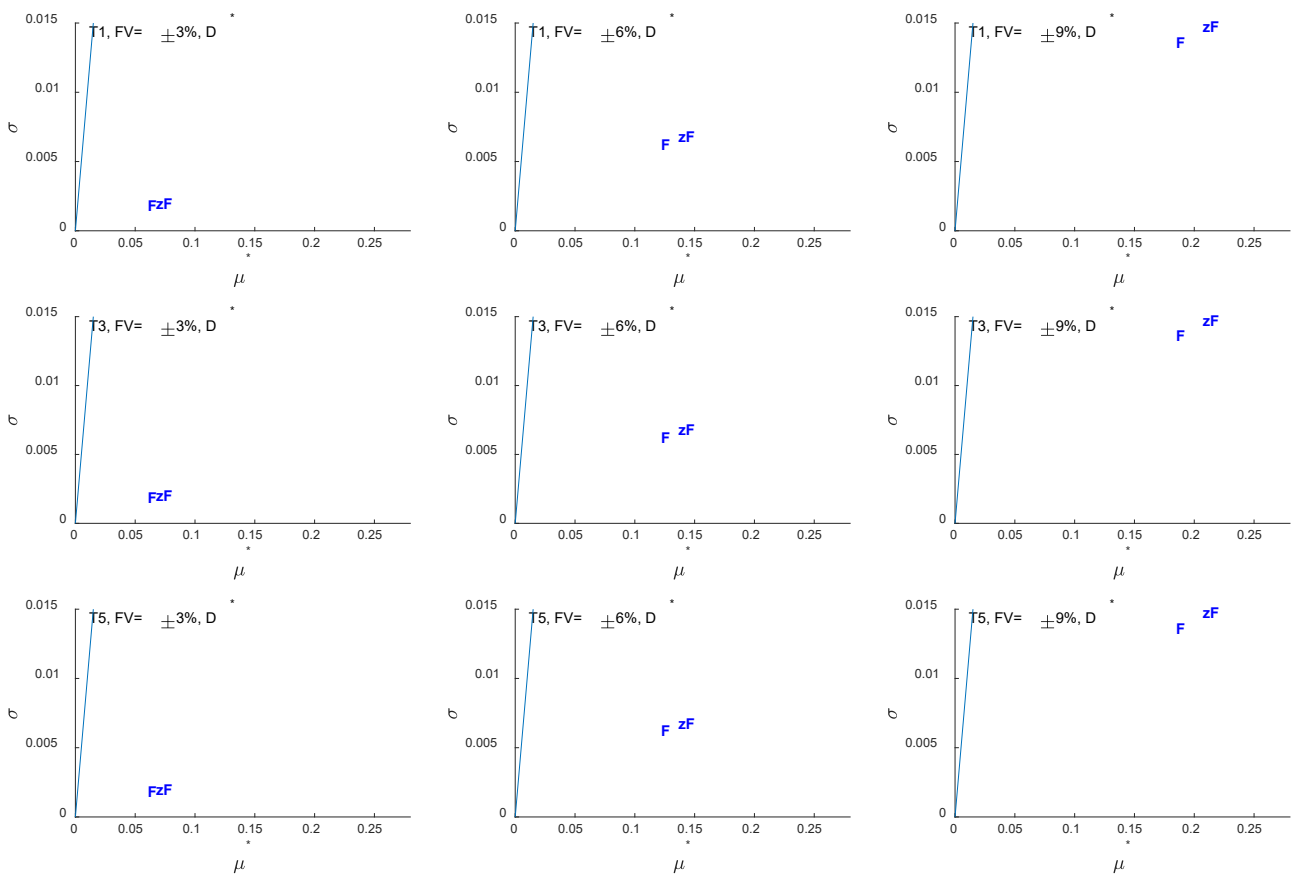


Fig. S1. Morris analysis of normalized top product flow (D^*) for tower configurations T1, T3, and T5 operating at specified product compositions ($x_D = 0.95, x_W = 0.05$) and three feed variability levels (FV).

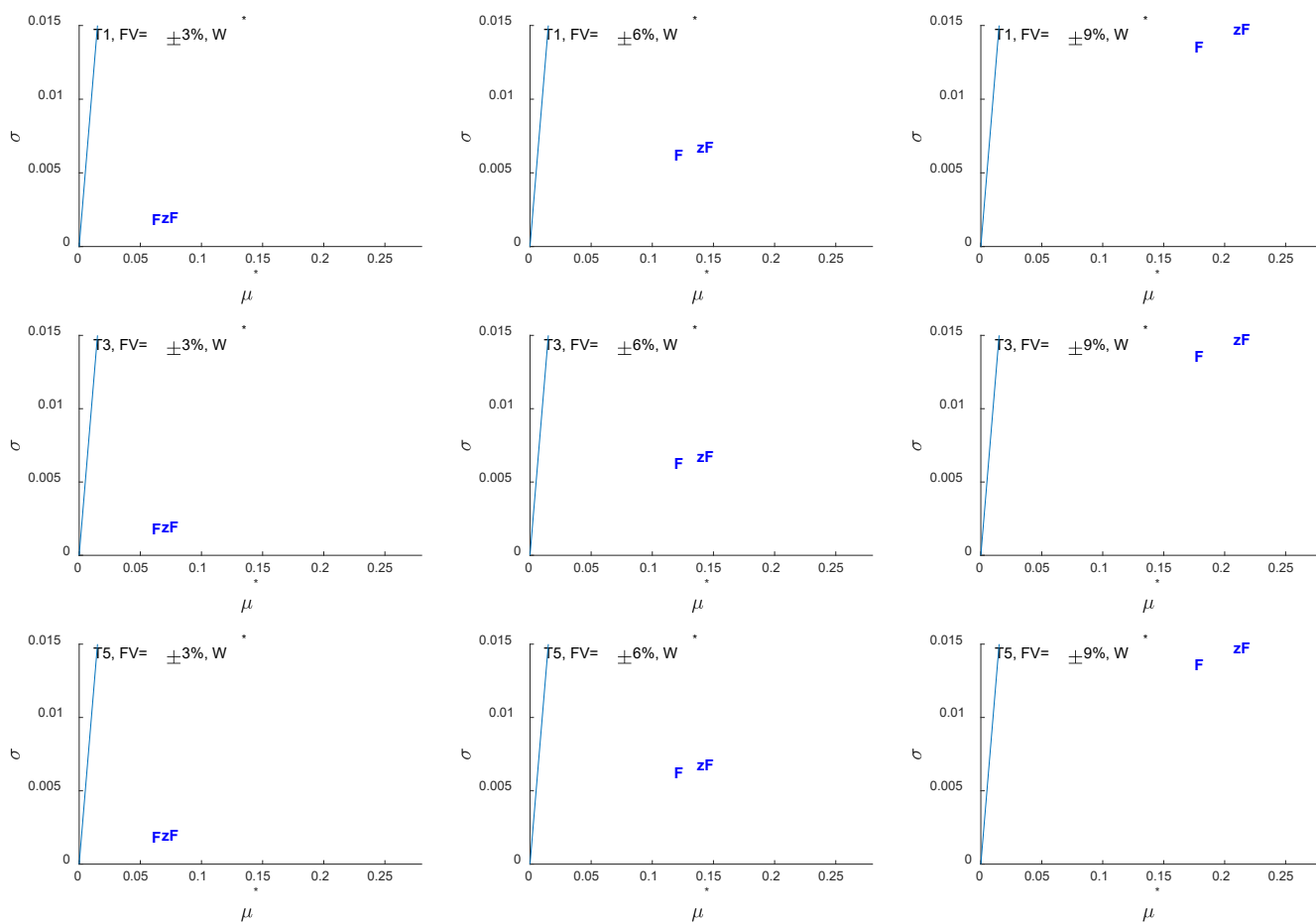


Fig. S2. Morris analysis of normalized bottom product flow (W_b) for tower configurations T1, T3, and T5 operating at specified product compositions ($x_D = 0.95, x_W = 0.05$) and three feed variability levels (FV).

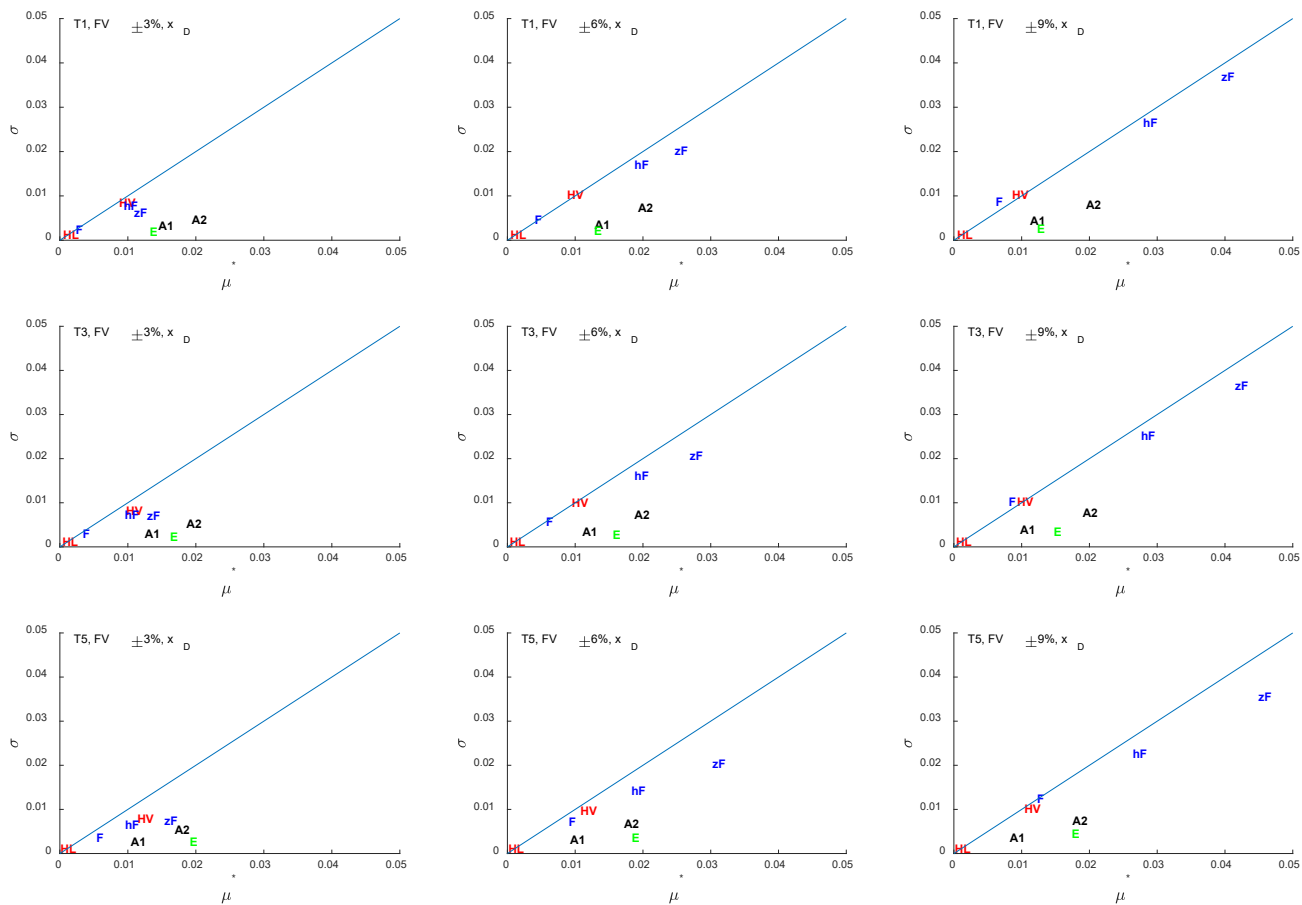


Fig. S3. Morris analysis of top composition (x_D) for tower configurations T1, T3 and T5 operating at reference reflux ratio and reboiler heat duty for three feed variability levels (FV).

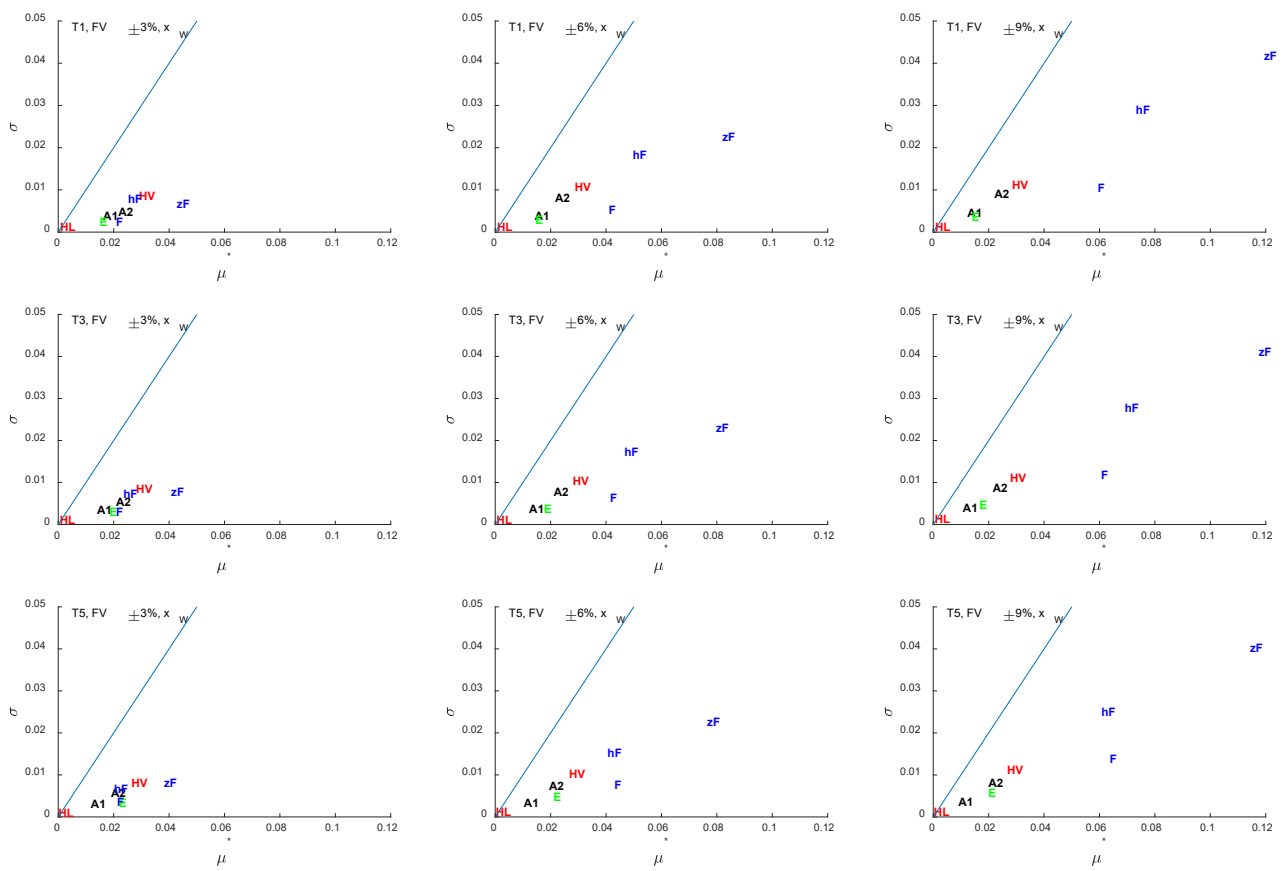


Fig. S4. Morris analysis of bottom composition (x_w) for tower configurations T1, T3 and T5 operating at reference reflux ratio and reboiler heat duty for three feed variability levels (FV).

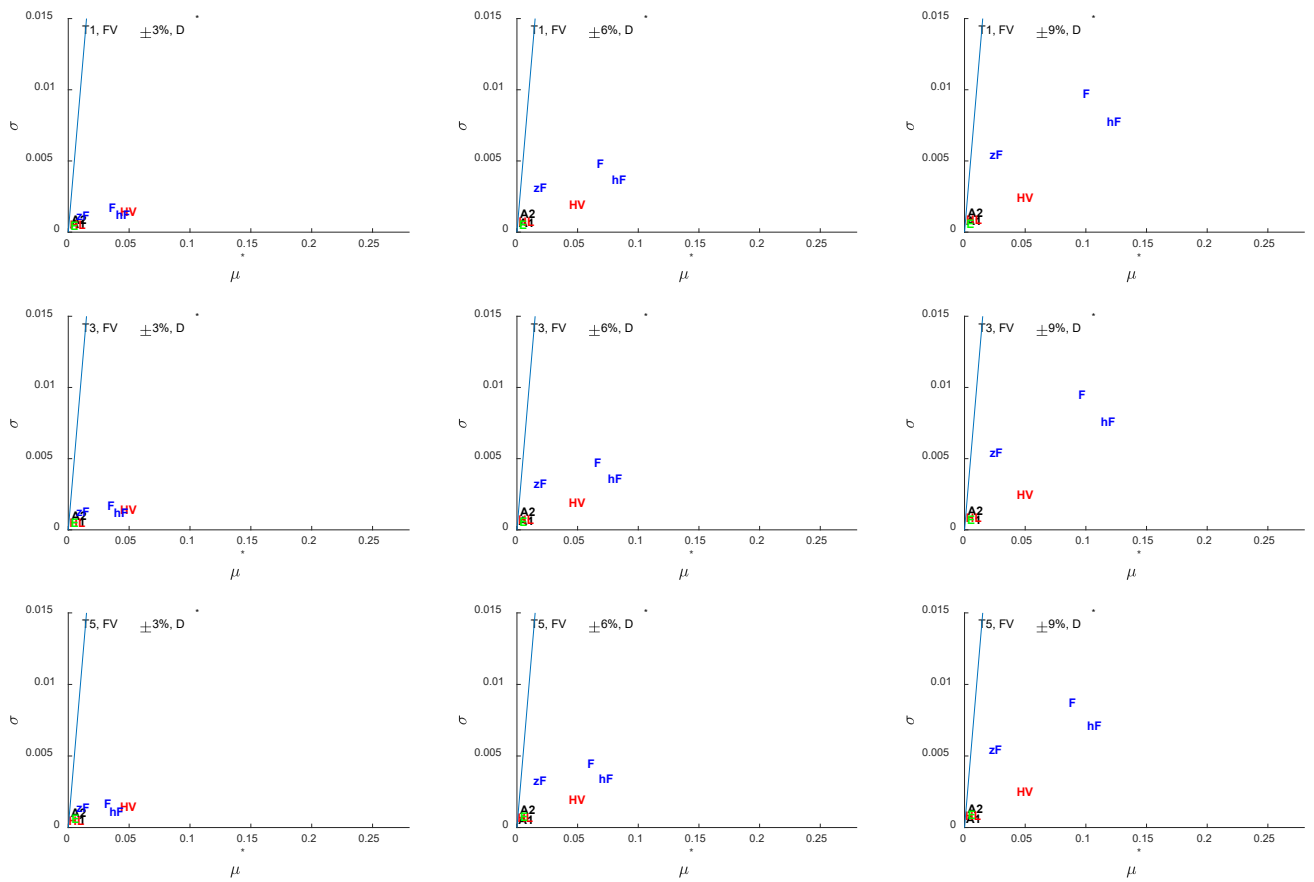


Fig. S5. Morris analysis of normalized top product flow (D^*) for tower configurations T1, T3 and T5 operating at reference reflux ratio and reboiler heat duty for three feed variability levels (FV).

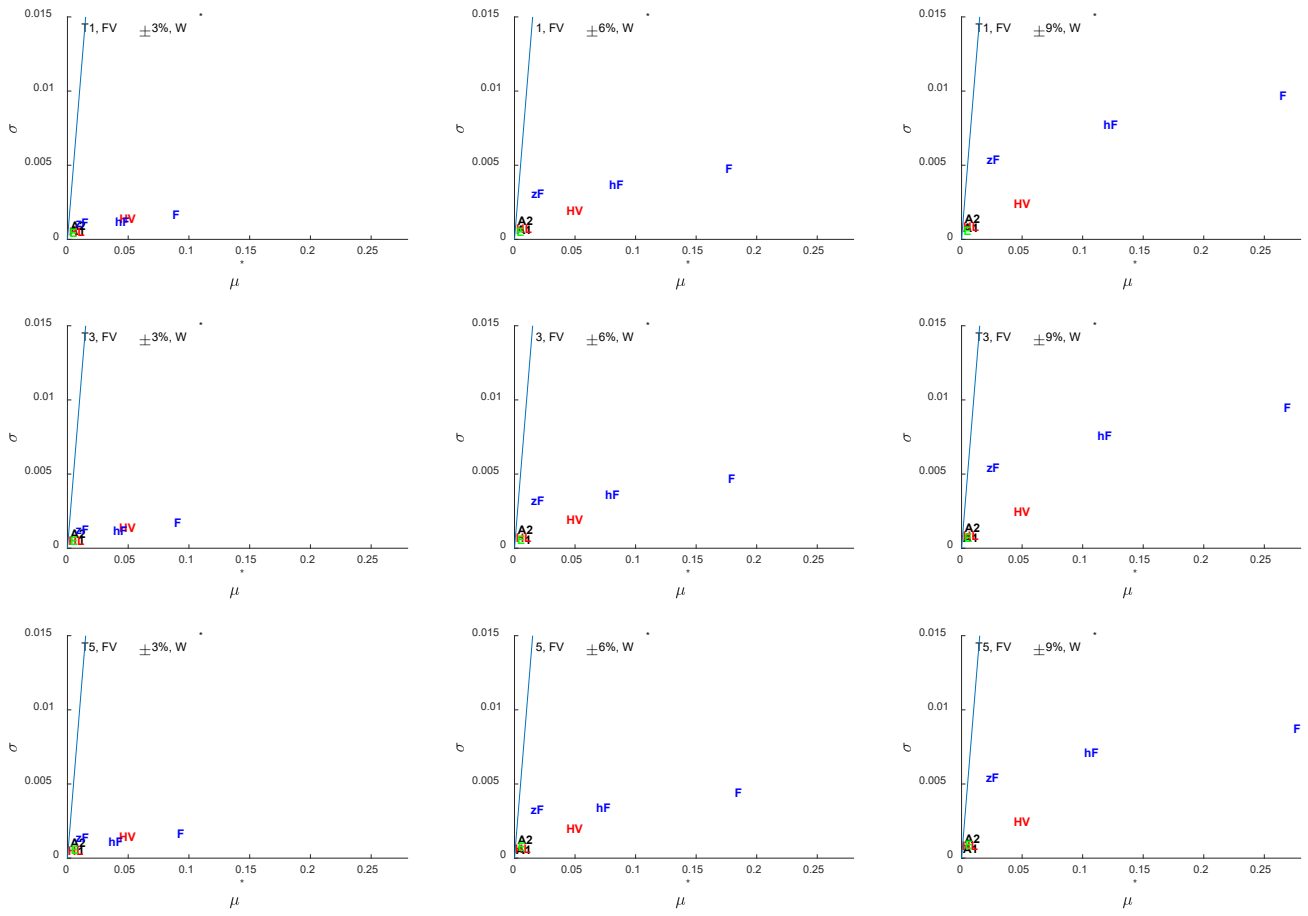


Fig. S6. Morris analysis of normalized bottom product flow (W^b) for tower configurations T1, T3 and T5 operating at reference reflux ratio and reboiler heat duty for three feed variability levels (FV).

Table S1. Sobol analysis of normalised reflux ratio and reboiler heat duty at specified product composition for tower configuration T3 and feed variability of $\pm 6\%$ ($n=1000$, $n_{boot} = 100$) discarding less relevant factors according Morris analysis

Variable	Factor	First index			Total index		
		orig.	min. c.i.	max. c.i.	orig.	min. c.i.	max. c.i.
Normalised reflux ratio, R^*	A1	<u>0.1602</u>	0.0670	0.2501	<u>0.1694</u>	0.1508	0.1904
	A2	<u>0.4434</u>	0.3817	0.5075	<u>0.4491</u>	0.4063	0.5047
	E	<u>0.3299</u>	0.2431	0.3955	<u>0.3603</u>	0.3233	0.3981
	F	-0.0125	-0.1216	0.0934	0.0071	0.0063	0.0082
	zF	-0.0278	-0.1429	0.0760	0.0120	0.0106	0.0135
	hF	-0.0196	-0.1264	0.0852	0.0112	0.0099	0.0125
Normalized reboiler heat duty, Q_B^*	A1	0.0168	-0.0801	0.1250	0.0976	0.1216	0.0168
	A2	<u>0.2330</u>	0.1663	0.3438	<u>0.2665</u>	0.3310	0.2330
	E	<u>0.1140</u>	0.0496	0.1904	<u>0.2120</u>	0.2618	0.1140
	F	0.0152	-0.0667	0.1047	0.0913	0.1126	0.0152
	zF	<u>0.1408</u>	0.0648	0.2276	<u>0.1846</u>	0.2418	0.1408
	hF	-0.0514	-0.1441	0.0484	0.0553	0.0699	-0.0514

Table S2. Sobol analysis of normalized top product flow (D^*) and bottom product flow (W^*) at specified product composition for tower configuration T3 and feed variability of $\pm 6\%$ (n=1000, nboot = 100)

Variable	Factor	First index			Total index		
		orig.	min. c.i.	max. c.i.	orig.	min. c.i.	max. c.i.
Normalised top product flow, D^*	A1	-0.0426	-0.1312	0.0641	0.0000	0.0000	0.0000
	A2	-0.0426	-0.1312	0.0641	0.0000	0.0000	0.0000
	HL	-0.0426	-0.1312	0.0641	0.0000	0.0000	0.0000
	HV	-0.0426	-0.1312	0.0641	0.0000	0.0000	0.0000
	E	-0.0426	-0.1312	0.0641	0.0000	0.0000	0.0000
	F	<u>0.4350</u>	0.3759	0.4938	<u>0.4407</u>	0.3917	0.4932
	zF	<u>0.5616</u>	0.5084	0.6122	<u>0.5665</u>	0.5075	0.6221
	hF	-0.0426	-0.1312	0.0641	0.0000	0.0000	0.0000
Normalized bottom product flow, W^*	A1	0.0241	-0.0575	0.1006	0.0000	0.0000	0.0000
	A2	0.0241	-0.0575	0.1006	0.0000	0.0000	0.0000
	HL	0.0241	-0.0575	0.1006	0.0000	0.0000	0.0000
	HV	0.0241	-0.0575	0.1006	0.0000	0.0000	0.0000
	E	0.0241	-0.0575	0.1006	0.0000	0.0000	0.0000
	F	<u>0.4308</u>	0.3871	0.4869	<u>0.4417</u>	0.3961	0.4896
	zF	<u>0.5560</u>	0.5070	0.6024	<u>0.5706</u>	0.5186	0.6147
	hF	0.0241	-0.0575	0.1006	0.0000	0.0000	0.0000

Table S3. Sobol analysis of normalized top product flow (D^*) and bottom product flow (W^*) at given operating conditions for tower configuration T3 and feed variability of $\pm 6\%$ (n=1000, nboot = 100)

Variable	Factor	First index			Total index		
		orig.	min. c.i.	max. c.i.	orig.	min. c.i.	max. c.i.
Normalised top product flow, D^*	A1	0.0087	-0.0753	0.0894	0.0003	0.0002	0.0003
	A2	0.0058	-0.0787	0.0873	0.0006	0.0005	0.0007
	HL	0.0091	-0.0749	0.0897	0.0001	0.0001	0.0001
	HV	<u>0.1677</u>	0.0866	0.2455	<u>0.1549</u>	0.1376	0.1733
	E	0.0087	-0.0765	0.0906	0.0004	0.0004	0.0005
	F	<u>0.3694</u>	0.3064	0.4281	<u>0.3558</u>	0.3215	0.3875
	zF	0.0224	-0.0560	0.0990	0.0177	0.0153	0.0193
	hF	<u>0.4615</u>	0.4123	0.5137	<u>0.4698</u>	0.4222	0.5172
Normalized bottom product flow, W^*	A1	-0.0187	-0.0901	0.0643	0.0001	0.0001	0.0001
	A2	-0.0181	-0.0884	0.0648	0.0002	0.0002	0.0002
	HL	-0.0198	-0.0912	0.0640	0.0000	0.0000	0.0000
	HV	0.0233	-0.0484	0.1000	0.0499	0.0437	0.0543
	E	-0.0190	-0.0897	0.0646	0.0001	0.0001	0.0001
	F	<u>0.7970</u>	0.7802	0.8183	<u>0.8172</u>	0.7518	0.8901
	zF	-0.0211	-0.0936	0.0561	0.0057	0.0050	0.0062
	hF	<u>0.1388</u>	0.0641	0.2139	<u>0.1513</u>	0.1377	0.1636